Journal of Computational Physics **159,** 58–89 (2000)
doi:10.1006/jcph.2000.6424, available online at http://www.idealibrary.com on IDEAL®

Conservation Properties of Unstructured Staggered Mesh Schemes

Blair Perot

Department of Mechanical and Industrial Engineering, University of Massachusetts, Box 32210-219, Engineering Laboratory, Amherst, Massachusetts 01003-2210
E-mail: perot@ecs.umass.edu

Received July 6, 1999

Classic Cartesian staggered mesh schemes have a number of attractive properties. They do not display spurious pressure modes and they have been shown to locally conserve, mass, momentum, kinetic energy, and circulation to machine precision. Recently, a number of generalizations of the staggered mesh approach have been proposed for unstructured (triangular or tetrahedral) meshes. These unstructured staggered mesh methods have been created to retain the attractive pressure aspects and mass conservation properties of the classic Cartesian mesh method. This work addresses the momentum, kinetic energy, and circulation conservation properties of unstructured staggered mesh methods. It is shown that with certain choices of the velocity interpolation, unstructured staggered mesh discretizations of the divergence form of the Navier–Stokes equations can conserve kinetic energy and momentum both locally and globally. In addition, it is shown that unstructured staggered mesh discretizations of the rotational form of the Navier–Stokes equations can conserve kinetic energy and circulation both locally and globally. The analysis includes viscous terms and a generalization of the concept of conservation in the presence of viscosity to include a negative definite dissipation term in the kinetic energy equation. These novel conserving unstructured staggered mesh schemes have not been previously analyzed. It is shown that they are first-order accurate on nonuniform two-dimensional unstructured meshes and second-order accurate on uniform unstructured meshes. Numerical confirmation of the conservation properties and the order of accuracy of these unstructured staggered mesh methods is presented.

Key Words: Navier–Stokes; staggered mesh; conservation; accuracy; unstructured.

1. INTRODUCTION

Strictly speaking, a staggered mesh scheme is any numerical scheme where variables are located at different points within the mesh. Many possible staggering schemes are possible. However, in this work we are interested in generalizations of a particular staggering scheme

0021-9991/00 $35.00

that dates originally to the work of Harlow and Welch [1]. They describe a scheme for regular Cartesian meshes where the pressure is located at cell centers but the velocity is distributed on the cell faces with horizontal velocity components prescribed at vertical faces and vertical velocity components prescribed at horizontal faces. This particular staggering scheme has been found to be especially attractive for simulations of incompressible flow and is widely used for this class of flows. The important property for incompressible flows is the fact that this scheme does not display spurious pressure modes. There is no red–black uncoupling of the pressure unknowns or a need for "stabilization" terms that damp pressure and velocity fluctuations.

Several properties beyond the ability to easily simulate incompressible flow make this method attractive for simulations of high Reynolds number flows. The method is typically very fast and uses minimal memory. In addition, it has been found that discretizations based on this staggering can conserve momentum, kinetic energy, and circulation [2]. Direct numerical simulations of turbulence have been successfully performed using the Cartesian staggered mesh discretization [3–5], and more recently the scheme has become popular for Large Eddy Simulation (LES) in complex geometries [6]. Furthermore, it has been demonstrated that local conservation of kinetic energy is particularly critical for large eddy simulations of turbulence [7], where it is observed that preserving the exact details of the small scale turbulent fluctuations is not nearly as important as preserving their overall kinetic energy and rate of dissipation. In two-dimensional turbulence, it is the enstrophy that becomes the important cascaded variable, and so it is likely in simulations of two-dimensional (geophysical) turbulence that conservation of circulation (vorticity) will be an important property of the numerical method.

Most numerical methods that are known to conserve kinetic energy or circulation, such as spectral methods or Cartesian staggered mesh schemes, require Cartesian meshes. If attention is restricted to methods that can be implemented on unstructured meshes and in complex geometries, the kinetic energy or circulation conservation properties are very restrictive. Mimetic discretizations on unstructured meshes which appear to be closely related to finite element methods can be constructed to globally conserve vorticity or enstropy or kinetic energy [8]. Galerkin finite element methods are known to be kinetic energy conserving (globally) on unstructured meshes. Unfortunately, experience with finite element methods for the LES simulation of turbulence indicates that they can also be expensive in that context [9]. In addition, finite element methods guarantee only *global* conservation of momentum and kinetic energy, the attractive local conservation properties often found with finite volume methods cannot be obtained. While finite volume methods do conserve mass, momentum, and *total* energy locally (usually by construction), in general, they do not conserve kinetic energy or circulation. In addition, standard finite volume methods are often subject to pressure instabilities and slow convergence at low Mach numbers. However, unstructured versions of the Harlow and Welch staggered mesh method hold significant potential for achieving local kinetic energy or vorticity conservation on unstructured meshes.

The staggered mesh method of Harlow and Welch was generalized to unstructured (triangular) meshes independently by Hall *et al.* [10] and by Nicolaides [11–13]. The works of Nicolaides provide extensive mathematical analysis of the method. These "dual mesh" or "covolume" methods take explicit advantage of the fact that every unstructured tetrahedral or triangular mesh (a Delaunay mesh) has an orthogonal or dual mesh associated with it (a Voronoi tessellation). An example of an unstructured mesh and its dual are shown in Fig. 1. The local mutual orthogonality of these meshes can be used to develop discretization

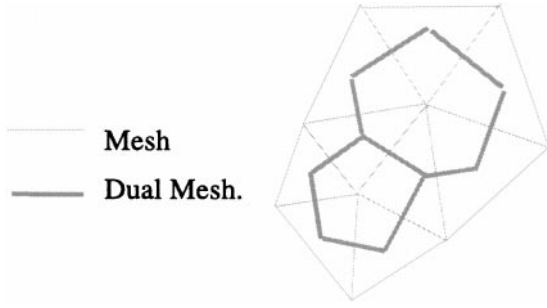

FIG. 1. Example of a two-dimensional unstructured triangular mesh and the associated Veronio dual mesh. The faces of the two meshes are always locally orthogonal.

operators that closely mimic their continuous counterparts. This allows a true inner product to be defined and important vector identities (such as $\nabla \cdot \nabla \times (\bullet) = 0$) to be maintained in a discrete sense. Similar, "mimetic" schemes for distorted Cartesian meshes have recently been proposed by Bertagnolio and Daube [14] and Hyman and Shashkov [15, 16].

It should be noted that while unstructured staggered mesh methods have numerous attractive mathematical properties, high-order accuracy is currently not one of them. Like the original Harlow and Welch discretization, the methods tend to be first-order accurate on nonuniform meshes. The issue of creating higher order unstructured staggered mesh schemes is not pursued herein. However, Morinishi *et al.* [17] have developed higher order staggered mesh schemes for Cartesian staggered grids, and Hyman *et al.* [18] have reported progress in developing high-order staggered mesh schemes for distorted quadrilateral meshes. Calculations of fluid evolution using unstructured staggered mesh schemes are reported in Refs. [19–21].

This work will evaluate the conservation properties of two different unstructured staggered mesh schemes. For the sake of clarity and brevity the analysis will be restricted to two dimensions, but it will be clear throughout the analysis that there are no fundamental hurdles to applying the analysis to three-dimensional discretizations. Section 2 looks at unstructured staggered mesh discretizations of the rotational form of the Navier–Stokes equations. The rotational form is attractive because it maps well to the staggered mesh approach and is inexpensive to implement. The rotational form is shown to conserve circulation and kinetic energy locally and globally. Section 3 looks at unstructured staggered mesh discretizations of the divergence form of the Navier–Stokes equations. The method is shown to conserve momentum and kinetic energy locally and globally. Numerical confirmation of these conservation properties is presented in Section 4. The accuracy of these conserving staggered mesh discretizations is analyzed in Section 5, and a short discussion is presented in Section 6.

2. ANALYSIS OF THE ROTATIONAL FORM

Unstructured staggered mesh methods have discretization operators that are ideally suited to a representation of the Navier–Stokes equations that is based on the vorticity. The following form of the incompressible Navier–Stokes equations will be referred to as the *rotational* form of the equations,

$$\frac{\partial \mathbf{u}}{\partial t} + (\omega \times \mathbf{u}) = -\nabla p^{\mathrm{d}} - \nabla \times (\nu \omega), \tag{1}$$

where $\mathbf{u}$ is the velocity vector, ω is the vorticity, $p^{\mathrm{d}} = p + \frac{1}{2}\mathbf{u}\cdot\mathbf{u}$ is the specific dynamic pressure, and ν is the kinematic viscosity. This equation assumes that viscosity is constant, but it is otherwise equivalent to other forms of the incompressible Navier–Stokes equations. Variable viscosity can be still be represented in rotational form but the extra term (involving second derivatives of viscosity) complicates the analysis unnecessarily. Despite the fact that this form of the Navier–Stokes equations is not common in textbooks it can be easily generalized to compressible flows and is a mathematically elegant way to view the equations. The convection term acts only perpendicularly to the velocity [$\mathbf{u}\cdot(\omega\times\mathbf{u}) = 0$], and the body force is now explicitly decomposed into its dilatational and solenoidal parts. This particular form of the Navier–Stokes equations is of interest because it appears to be inherently suited to the staggered mesh discretization. The classic staggered mesh method of Harlow and Welch can be rearranged to look like a discretization of Eq. (1).

2.1. *Unstructured Discretization of the Rotational Form*

Staggered mesh schemes, either structured or unstructured, are concerned with the evolution of the normal velocity component, u, at the faces of the mesh cells. In two dimensions the staggered mesh discretization of the rotational form of the normal momentum equation at each cell face is

$$W_{\mathrm{f}}A_{\mathrm{f}}\frac{u^{n+1}-u^{n}}{\Delta t} - \frac{1}{2}(\omega_{\mathrm{n1}}v_{\mathrm{n1}}+\omega_{\mathrm{n2}}v_{\mathrm{n2}})W_{\mathrm{f}}A_{\mathrm{f}} = -\left(p^{\mathrm{d}}_{\mathrm{c2}}-p^{\mathrm{d}}_{\mathrm{c1}}\right)A_{\mathrm{f}} - (\nu_{\mathrm{n2}}\omega_{\mathrm{n2}}-\nu_{\mathrm{n1}}\omega_{\mathrm{n1}})W_{\mathrm{f}}, \quad (2)$$

where W_{f}, is the distance (or width) between neighboring cell circumcenters, A_{f} is the face area, u is the normal velocity component as the face, ω_{n} is the vorticity at the mesh nodes, and $p^{\mathrm{d}}_{\mathrm{c}}$ is the specific dynamic pressure at cell circumcenters. In two dimensions the face area A_{f}, is really just a length (the distance between the face end points) times a unit depth into the plane. The convention which is assumed here is that the normal vector points from cell c1 to cell c2, the tangential vector points from node n1 to node n2, and the tangential vector is oriented 90° counterclockwise to the normal vector (see Fig. 2). The orthogonality of the normal and tangential vectors can always be obtained if the cell positions are located at the cell circumcenters. The methods discussed in this manuscript assume that the cells have a circumcenter. This is true of meshes that consist of collections of

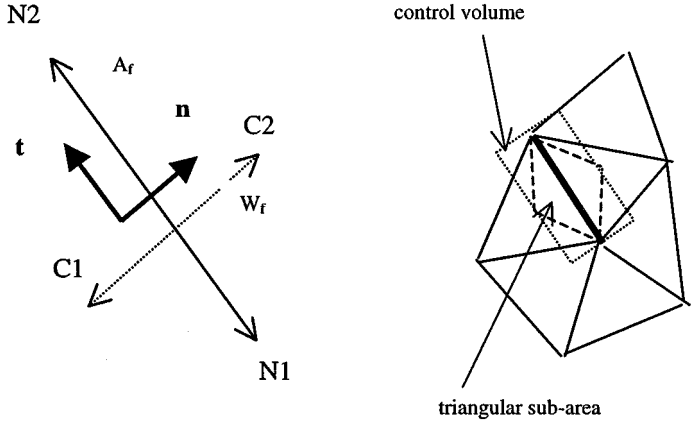

FIG. 2. Notation for a cell face and the face in the context of the larger mesh.

triangles, rectangles, and symmetric trapezoids (and their three-dimensional counterparts), but is not true of a mesh composed of arbitrary quadrilaterals (or hexahedra). Extension of the staggered mesh method to arbitrary quadrilaterals is discussed in Ref. [15]. Arbitrary quadrilaterals force some of the discretization operators to be implicit, which complicates the analysis. While the following proofs require the presence of cell circumcenters, they do not require that the cell circumcenters be located within the cell itself or that the mesh be a Delaunay tessellation. Highly distorted grids can impact the accuracy of the unstructured staggered mesh method as discussed in [16] but do not affect its conservation properties. The test cases in Section 4 use meshes in which a significant fraction of the cell circumcenters lie outside the respective cell.

In this notation, the velocity component normal to the cell face is u, and the tangential velocity component at the face is v. These local velocity components should not be confused with the x and y components of the velocity vector (which are given by u_x and u_y). The convective term is actually calculated at the nodes and then averaged to the face. In two dimensions, the vorticity is assumed to point out of the two-dimensional plane. For convenience, we have represented the entire gradient term using a dynamic pressure, p^{d}. Boundary faces are discretized in exactly the same manner, with the external cell (c2) located infinitesimally close to the boundary face. The time level has been dropped from all but the time derivative term for simplicity. However, the time levels are not necessarily arbitrary and some implications of various time level choices are discussed in the text.

If Eq. (2) is divided by $W_{\mathrm{f}}A_{\mathrm{f}}$, the discretization can be viewed as an unstructured finite difference approximation to the normal momentum equation. However, it can also be interpreted as a control volume approximation on a rectangular control volume with width W_{f} and height A_{f}. Note that the control volumes overlap and their total area will be exactly twice the area of the entire domain. This can be seen by the fact that each control volume rectangle is exactly twice as big as the two subtriangles associated with each face (see Fig. 2). The doubling of the total control volume area makes sense since the method solves for only half the velocity components. While the use of overlapping control volumes is perhaps troubling at first, it will be clear upon completion of the text that this is indeed a legitimate approach. If a regular Cartesian mesh is used it can be shown that this discretization is equivalent to the Harlow and Welch staggered mesh scheme. The accuracy of a similar staggered mesh scheme (with a different convection term) was analyzed by Nicolaides [11] and shown to be second-order accurate on uniform unstructured two-dimensional meshes.

Analysis of the method is made somewhat easier if the discrete equations are written in operator form,

$$W_{\mathrm{f}}A_{\mathrm{f}}\frac{u^{n+1}-u^{n}}{\Delta t} - W_{\mathrm{f}}A_{\mathrm{f}}\,\mathbf{AVG}(\omega_{\mathrm{n}}v_{\mathrm{n}}) = -A_{\mathrm{f}}\,\mathbf{GRAD}\left(p_{\mathrm{c}}^{\mathrm{d}}\right) - W_{\mathrm{f}}\,\mathbf{CURL}(\nu_{\mathrm{n}}\omega_{\mathrm{n}}), \qquad (3)$$

where **AVG** is the averaging operator, **GRAD** is the gradient operator, and **CURL** is the curl operator. These operators are nonsquare, sparse matrices. The nonzero entries in the difference operators **GRAD** and **CURL** are either plus or minus one. The gradient and curl operators have a similar function to their continuous counterparts but differ slightly in that these matrices have been stripped of their geometric information such as heights and widths. It can be shown [22] that $(\mathbf{CURL})^{\mathrm{T}}\ \mathbf{GRAD}(\bullet) = 0$, which is the analog of $\nabla \times \nabla(\bullet) = 0$. We will not use this fact in what follows but it highlights an important point: the staggered mesh operators have many properties that mimic their continuous counterparts [23]. What will be used in the conservation proofs will be discrete integration by parts analogs for

these discrete operators. Discrete integration by parts will allow us to develop proofs of conservation that proceed very much like their continuous counterparts.

2.2. *Conservation of Kinetic Energy: Rotational Form*

For the continuous Navier–Stokes equations, kinetic energy conservation is derived by taking a dot product of the momentum equation with the velocity vector and using integration by parts. If we continue to consider an incompressible fluid then kinetic energy conservation is given by the equation,

$$\frac{\partial\left(\frac{1}{2}\mathbf{u}\cdot\mathbf{u}\right)}{\partial t}+\nabla\cdot\left[\mathbf{u}\left(\frac{1}{2}\mathbf{u}\cdot\mathbf{u}\right)\right]=-\nabla\cdot(p\mathbf{u})+\nabla\cdot(\nu\mathbf{u}\times\omega)-\nu\omega\cdot\omega, \tag{4}$$

where $\frac{1}{2}\mathbf{u}\cdot\mathbf{u}$ is the specific kinetic energy of the fluid. Strictly speaking, conservation applies only in the inviscid limit of zero viscosity. In the presence of viscosity the last term is a negative semidefinite sink term that causes the total kinetic energy to decay monotonically in the absence of external forces. The discrete system will actually mimic this more general notion of kinetic energy conservation. It will satisfy a discrete equation analogous to the continuous equation above, where total kinetic energy decreases due to a single dissipation term which is equal to the product of the discrete enstrophy and viscosity.

The primary difficulty of analyzing the conservation properties of staggered mesh methods is the fact that only the normal component of the velocity vector at the mesh faces is discretized. The choice of velocity interpolation is then intimately associated with how velocity-dependent quantities like momentum and kinetic energy are defined. During the course of the proof we must also determine how best these quantities should be defined.

To show discrete kinetic energy conservation we multiply each equation for the normal velocity at the face by the half-time normal velocity, $u^{n+1/2}$, at the face and then sum over the faces. Note that in the discrete derivation there is no dot product, only the normal momentum equation and normal velocity are involved. Discrete conservation of kinetic energy will be derived by showing that a discrete form of integration by parts can be applied to each term of the normal momentum equation. Then it will be shown that this portion of the kinetic energy (that due to $\frac{1}{2}u^2$ summed over all cell faces) is an approximation for the full kinetic energy within each mesh cell.

If the summation is performed over all the faces of a single control volume then the following proof is a statement of local kinetic energy conservation. It states that the change in kinetic energy within the control volume is only a result of fluxes through the control volume surfaces and viscous dissipation. If the summation is performed over all the faces in a mesh (including the boundary faces) then the interior fluxes cancel out and the resulting proof is a statement of global conservation. Global conservation states that the change in total kientic energy is due only to fluxes through the boundary of the domain and the total viscous dissipation inside the domain.

Discrete conservation starts with the following equation:

$$\begin{aligned}&\sum^{\text{faces}} u^{n+1/2}W_{\mathrm{f}}A_{\mathrm{f}}\frac{u^{n+1}-u^{n}}{\Delta t}-\sum^{\text{faces}} u^{n+1/2}W_{\mathrm{f}}A_{\mathrm{f}}\,\mathbf{AVG}(\omega_{\mathrm{n}}v_{\mathrm{n}})\\&\quad=-\sum^{\text{faces}} u^{n+1/2}A_{\mathrm{f}}\,\mathbf{GRAD}\left(p_{\mathrm{c}}^{\mathrm{d}}\right)-\sum^{\text{faces}} u^{n+1/2}W_{\mathrm{f}}\,\mathbf{CURL}(v_{\mathrm{n}}\omega_{\mathrm{n}}).\end{aligned} \tag{5}$$

The goal will be to move $u^{n+1/2}$ within each of the operators (including the time derivative) in order to derive a discrete analog of Eq. (4). Each term in this equation is analyzed below.

2.2.1. Time derivative. If we require that $u^{n+1/2} = \frac{1}{2}(u^{n+1} + u^n)$, then the time derivative term can be simplified as follows:

$$\sum^{\text{faces}} W_f A_f u^{n+1/2} \frac{u^{n+1} - u^n}{\Delta t} = \sum^{\text{faces}} W_f A_f \frac{1}{2}(u^{n+1} + u^n) \frac{u^{n+1} - u^n}{\Delta t}$$
$$= \sum^{\text{faces}} W_f A_f \frac{\left(\frac{1}{2}uu\right)^{n+1} - \left(\frac{1}{2}uu\right)^n}{\Delta t}. \tag{6}$$

Remember that the width W_f is the distance between the neighboring two cell circumcenters (Fig. 2). On boundary faces W_f is the distance from the interior cell circumcenter to the face midpoint. The width can be decomposed into two parts, each representing the distance from the face midpoint to one of the cell circumcenters; $W_f = W_f^{C1} + W_f^{C2}$. On boundary faces the second part is zero. With this notation, the sum over faces can be recast as summation over the cells,

$$= \sum^{\text{faces}} \left(W_f^{C1} + W_f^{C2}\right) A_f \frac{\left(\frac{1}{2}uu\right)^{n+1} - \left(\frac{1}{2}uu\right)^n}{\Delta t} = \sum^{\text{cells}} \left[\sum_{\text{faces}}^{\text{cell}} W_f^C A_f \frac{\left(\frac{1}{2}uu\right)^{n+1} - \left(\frac{1}{2}uu\right)^n}{\Delta t} \right], \tag{7}$$

where the term in square brackets can be identified as the change in discrete kinetic energy within the cell. The discrete kinetic energy in a cell is therefore defined by the expression

$$K = \frac{1}{V_c} \sum_{\text{faces}}^{\text{cell}} W_f^C A_f \left(\frac{1}{2}uu\right), \tag{8}$$

where V_c is the volume of the cell. Note that the summation involves only the "kinetic energy" associated with the normal velocity components. Also note that the summation is effectively a volume weighted average but that the weights add up to 2, so the weights account for the fact that only part of the total kinetic energy at each face is being averaged. It is shown in Section 5.2 that the average described above is a first-order accurate approximation for the kinetic energy in an arbitrary two-dimensional cell.

With the discrete kinetic energy defined in this way the time derivative term for the discrete kinetic energy equation can be written as

$$= \sum^{\text{cells}} V_c \frac{K^{n+1} - K^n}{\Delta t} \tag{9}$$

This equation is valid for a collection of cells or an individual mesh cell. Note that for unsteady flows kinetic energy conservation requires using a standard time derivative approximation $(u^{n+1} - u^n)/\Delta t$ and the midpoint rule for the half-time velocity $u^{n+1/2} = \frac{1}{2}(u^n + u^{n+1})$. Setting $u^{n+1/2} = u^n$ in the derivation or using a second-order backward difference for the time derivative results in a first-order, but not necessarily positive, definite approximation for the kinetic energy at the next time level.

2.2.2. Convective term. Here we will attempt to construct a discrete version of the convective term, $(\omega \times \mathbf{u}) \cdot \mathbf{n}$, which gives no contribution to the discrete kinetic energy equation since this term does not contribute in the continuous kinetic energy equation.

The convective term in the kinetic energy is given by

$$\sum^{\text{faces}} u^{n+1/2} W_f A_f \, \mathbf{AVG}(\omega_n v_n) \equiv \sum^{\text{faces}} u^{n+1/2} W_f A_f \frac{1}{2}(\omega_{n1} v_{n1} + \omega_{n2} v_{n2}), \tag{10}$$

where ω_n is the vorticity at the node. The component of velocity that is used is the component of velocity oriented 90° counterclockwise to the face normal vector. This is precisely written as

$$= \sum^{\text{faces}} u^{n+1/2} W_f A_f \frac{1}{2}[\mathbf{n}_f \times (\omega_{n1}\mathbf{v}_{n1} + \omega_{n2}\mathbf{v}_{n2})] \cdot \mathbf{z}, \tag{11}$$

where $\mathbf{z}$ is the unit vector pointing out of the two-dimensional plane. The summation above can be recast as a summation over mesh nodes:

$$= \sum^{\text{nodes}} \omega_n \mathbf{z} \cdot \left(\left[\sum_{\text{faces}}^{\text{node}} u^{n+1/2} W_f A_f \frac{1}{2} \mathbf{n}_f \right] \times \mathbf{v}_n \right). \tag{12}$$

The cross product term in large brackets is the term of critical interest. If it is desired that this term be identically zero for arbitrary flows then the term in square brackets must be proportional to the velocity at the nodes ($\mathbf{v}_n$). This can be achieved by defining the node velocity as

$$\mathbf{v}_n = \frac{1}{A_n} \sum_{\text{faces}}^{\text{node}} u^{n+1/2} W_f A_f \frac{1}{2} \mathbf{n}_f, \tag{13}$$

where A_n is the area associated with each node (see Fig. 1). Section 5.3 shows that this is a first-order approximation for the velocity on uniform meshes. However, on nonuniform meshes it is found that this is only a zeroth-order approximation for the velocity at the nodes. So while this discretization conserves kinetic energy, it has sacrificed convergence to the Navier–Stokes equations. While the error is shown to be small in Section 5.5, it is nonetheless disconcerting. A modified discretization of the convective term is presented below which leads to a first-order accurate velocity at the nodes.

2.2.3. Modified convective term. The analysis in Section 5.3 which shows that the velocity defined by Eq. (13) is zeroth-order accurate for arbitrary meshes also shows how to improve the accuracy to first order. The first-order expression for the node velocity is similar to Eq. (13).

$$\mathbf{v}_n = \frac{1}{A_n} \sum_{\text{faces}}^{\text{node}} \hat{u}^{n+1/2} W_f \mathbf{z} \times (\mathbf{x}_f^* - \mathbf{x}_n), \tag{14}$$

where $\mathbf{x}_f^*$ is the face position midway between the two neighboring cell circumcenters, and $\hat{u}$ is the component of velocity normal to the face and oriented in a counterclockwise direction with respect to the node. For uniform meshes, $\mathbf{x}_f^*$ equals $\mathbf{x}_f$, so $\mathbf{z} \times (\mathbf{x}_f^* - \mathbf{x}_n) = \pm\frac{1}{2} A_f \mathbf{n}_f$ and

Eq. (13) equals Eq. (14). Working backward from Eq. (14), this implies that we would like Eq. (12) to have the form

$$\sum^{\text{nodes}} \omega_{\text{n}} \mathbf{z} \cdot \left(\left[\sum^{\substack{\text{node} \\ \text{faces}}} \hat{u}^{n+1/2} W_{\text{f}} \mathbf{z} \times (\mathbf{x}_{\text{f}}^* - \mathbf{x}_{\text{n}}) \right] \times \mathbf{v}_{\text{n}} \right). \tag{15}$$

Recasting this as a summation over faces gives

$$= \sum^{\text{faces}} \hat{u}^{n+1/2} W_{\text{f}} [\{\mathbf{z} \times (\mathbf{x}_{\text{f}}^* - \mathbf{x}_{\text{n1}})\} \times \mathbf{v}_{\text{n1}} \omega_{\text{n1}} - \{\mathbf{z} \times (\mathbf{x}_{\text{f}}^* - \mathbf{x}_{\text{n2}})\} \times \mathbf{v}_{\text{n2}} \omega_{\text{n2}}] \cdot \mathbf{z}, \tag{16}$$

which simplifies to

$$= \sum^{\text{faces}} u^{n+1/2} W_{\text{f}} [(\mathbf{x}_{\text{f}}^* - \mathbf{x}_{\text{n1}}) \cdot \mathbf{v}_{\text{n1}} \omega_{\text{n1}} - (\mathbf{x}_{\text{f}}^* - \mathbf{x}_{\text{n2}}) \cdot \mathbf{v}_{\text{n2}} \omega_{\text{n2}}]. \tag{17}$$

This implies that the rotational form of the convection term $(\omega \times \mathbf{u}) \cdot \mathbf{n}$ should be discretized as

$$= W_{\text{f}} [(\mathbf{x}_{\text{f}}^* - \mathbf{x}_{\text{n1}}) \cdot \mathbf{v}_{\text{n1}} \omega_{\text{n1}} - (\mathbf{x}_{\text{f}}^* - \mathbf{x}_{\text{n2}}) \cdot \mathbf{v}_{\text{n2}} \omega_{\text{n2}}], \tag{18}$$

rather than using Eq. (11). Note that Eq. (10) still holds but we now have a new definition for the tangential velocity, v_{n}. Section 5.3 shows that Eq. (18) is still a first-order approximation for the convection term.

Note that conservation of kinetic energy requires that the velocity in the convection term should be evaluated at the half time level, but there are no restrictions on the time level of the vorticity.

2.2.4. Gradient term. This Section will show how the **GRAD** operator satisfies a discrete version of the chain rule analogous to $\mathbf{u} \cdot \nabla \phi = \nabla \cdot (\mathbf{u}\phi) - \phi(\nabla \cdot \mathbf{u})$. The gradient term in the discrete energy equation actually contains two terms, a pressure contribution and a kinetic energy contribution. The kinetic energy portion will eventually become the convection of kinetic energy. The pressure portion becomes the traditional pressure work term. If we ignore the initial minus sign for now, the gradient term in the kinetic energy can be rearranged as follows:

$$\sum^{\text{faces}} u^{n+1/2} A_{\text{f}} \, \mathbf{GRAD}\big(p_{\text{c}}^{\text{d}}\big) = \sum^{\text{faces}} u^{n+1/2} A_{\text{f}} \big[\big(p_{\text{c2}}^{\text{d}} - p_{\text{f}}^{\text{d}}\big) - \big(p_{\text{c1}}^{\text{d}} - p_{\text{f}}^{\text{d}}\big)\big]. \tag{19}$$

Note that the normal velocity component has an orientation (from C1 to C2), and the dynamic pressure at the cell faces p_{f}^{d} has been introduced. This latter step is not necessary, and the proof can proceed by simply remembering that at boundary faces of the domain the outer cell (C2) position is the same as the face position (so $p_{\text{C2}}^{\text{d}} = p_{\text{f}}^{\text{d}}$). However, the current construction makes the chain rule analogy mentioned above more obvious. The summation over faces can now be rewritten as a summation over cells,

$$= \sum^{\text{cells}} \sum^{\substack{\text{cell} \\ \text{faces}}} \hat{u}^{n+1/2} A_{\text{f}} \big(p_{\text{f}}^{\text{d}} - p_{\text{c}}^{\text{d}}\big) = \sum^{\text{cells}} \sum^{\substack{\text{cell} \\ \text{faces}}} p_{\text{f}}^{\text{d}} \hat{u}^{n+1/2} A_{\text{f}} - \sum^{\text{cells}} p_{\text{c}}^{\text{d}} \left[\sum^{\substack{\text{cell} \\ \text{faces}}} \hat{u}^{n+1/2} A_{\text{f}} \right], \tag{20}$$

where the normal velocity $\hat{u}$ is defined to be the normal component of velocity that points *outward* relative to the cell in question (rather than from C1 to C2). The term in square brackets is the discrete version of the velocity divergence. This derivation shows that in operator notation we can write

$$\mathbf{DIV}\left(uA_{\mathrm{f}}p_{\mathrm{f}}^{\mathrm{d}}\right) = \sum^{\substack{\text{cell}\\ \text{faces}}} uA_{\mathrm{f}}\,\mathbf{GRAD}\left(p_{\mathrm{c}}^{\mathrm{d}}\right) + p_{\mathrm{c}}^{\mathrm{d}}\,\mathbf{DIV}(uA_{\mathrm{f}}), \tag{21}$$

where $\mathbf{DIV} = \mathbf{GRAD}^{\mathrm{T}}$ is the discrete divergence operator. The summation over cell faces is required in the discrete version, because the discrete operators do not operate on vector quantities, the vector nature of the continuous analog is implicitly obtained by summation over the components oriented in different directions.

If the solution method satisfies the discrete continuity equation, $\mathbf{DIV}(uA_{\mathrm{f}}) = 0$, then the gradient term in the kinetic energy equation becomes

$$= \sum^{\text{cells}} \sum^{\substack{\text{cell}\\ \text{faces}}} p_{\mathrm{f}}^{\mathrm{d}}\hat{u}^{n+1/2}A_{\mathrm{f}} = \sum^{\text{cells}} \sum^{\substack{\text{cell}\\ \text{faces}}} p_{\mathrm{f}}\hat{u}^{n+1/2}A_{\mathrm{f}} + \sum^{\text{cells}} \sum^{\substack{\text{cell}\\ \text{faces}}} \left(\frac{1}{2}\mathbf{u}\cdot\mathbf{u}\right)_{\mathrm{f}} \hat{u}^{n+1/2}A_{\mathrm{f}}, \tag{22}$$

which is a pressure work term and a kinetic energy convection term. Note that when the summation occurs over many cells the contributions from faces with two cells (interior faces) cancel out because the outward pointing velocity $\hat{u}^{n+1/2}$ is equal and opposite for the two cells. Only boundary faces (with one cell contribution) survive, so this summation can be further simplified to

$$= \sum^{\substack{\text{boundary}\\ \text{faces}}} p_{\mathrm{f}}\hat{u}^{n+1/2}A_{\mathrm{f}} + \sum^{\substack{\text{boundary}\\ \text{faces}}} \left(\frac{1}{2}\mathbf{u}\cdot\mathbf{u}\right)_{\mathrm{f}} \hat{u}^{n+1/2}A_{\mathrm{f}}, \tag{23}$$

where $\hat{u}^{n+1/2}$ always points out of the domain. This indicates that the gradient term neither creates nor destroys discrete kinetic energy; it only moves it around. The same is true in the continuous case.

2.2.5. Viscous term. This Section will show that the **CURL** operator also satisfies a discrete version of the chain rule for differentiation. It is analogous to $-\mathbf{u}\cdot(\nabla\times\nu\omega) = \nabla\cdot(\mathbf{u}\times\nu\omega) - \nu\omega\cdot(\nabla\times\mathbf{u})$. The viscous term in the kinetic energy equation is

$$-\sum^{\text{faces}} u^{n+1/2}W_{\mathrm{f}}\,\mathbf{CURL}(\nu_{\mathrm{n}}\omega_{\mathrm{n}}) = \sum^{\text{faces}} u^{n+1/2}W_{\mathrm{f}}(\nu_{\mathrm{n}1}\omega_{\mathrm{n}1} - \nu_{\mathrm{n}2}\omega_{\mathrm{n}2}). \tag{24}$$

This expression can be converted into a summation over mesh nodes,

$$= -\sum^{\text{nodes}} \nu_{\mathrm{n}}\omega_{\mathrm{n}} \sum^{\substack{\text{node}\\ \text{faces}}} \hat{u}^{n+1/2}W_{\mathrm{f}}, \tag{25}$$

where $\hat{u}$ is the velocity component normal to the face and pointing counterclockwise with respect to the node in question. If a node is in the interior of the domain, then the summation over node faces is a discrete approximation for the vorticity at the node (times the node area). On boundary nodes, the discrete vorticity must be completed by integrating the velocity around the boundary faces connected to the boundary node. Define the vorticity at a node

using a discrete version of Stokes theorem,

$$\omega_{\mathrm{n}}^{n+1/2} A_{\mathrm{n}} = \sum_{\substack{\text{node}\\ \text{faces}}} \hat{u}^{n+1/2} W_{\mathrm{f}} + \mathbf{u}_{\mathrm{n}} \cdot \left(\mathbf{t}_{\mathrm{bf}\,1} \frac{1}{2} A_{\mathrm{bf}\,1} + \mathbf{t}_{\mathrm{bf}\,2} \frac{1}{2} A_{\mathrm{bf}\,2} \right), \tag{26}$$

where $\mathbf{t}$ is the tangential vector on the boundary faces (oriented counterclockwise). The last term is necessary only for boundary nodes, and the normal vector is assumed to point outward at boundary faces. Then the viscous term becomes

$$= - \sum^{\text{nodes}} \nu_{\mathrm{n}} \omega_{\mathrm{n}} \omega_{\mathrm{n}}^{n+1/2} A_{\mathrm{n}} + \sum^{\substack{\text{boundary}\\ \text{nodes}}} \nu_{\mathrm{n}} \omega_{\mathrm{n}} \mathbf{u}_{\mathrm{n}} \cdot \left(\mathbf{t}_{\mathrm{bf}\,1} \frac{1}{2} A_{\mathrm{bf}\,1} + \mathbf{t}_{\mathrm{bf}\,2} \frac{1}{2} A_{\mathrm{bf}\,2} \right). \tag{27}$$

The second term can be converted to a summation over boundary faces:

$$= - \sum^{\text{nodes}} \nu_{\mathrm{n}} \omega_{\mathrm{n}} \omega_{\mathrm{n}}^{n+1/2} A_{\mathrm{n}} + \sum^{\substack{\text{boundary}\\ \text{faces}}} A_{\mathrm{f}} \frac{1}{2} \mathbf{t}_{\mathrm{f}} \cdot \sum^{\substack{\text{faces}\\ \text{nodes}}} \nu_{\mathrm{n}} \omega_{\mathrm{n}} \mathbf{u}_{\mathrm{n}}. \tag{28}$$

The first term is an approximation for dissipation in the domain. The second term is an approximation for $\nabla \cdot (\nu \mathbf{u} \times \omega)$ in the domain. The approximation for $\mathbf{u} \times \omega$ at the faces is the same as that used for the convective term earlier. These terms correspond directly to what is found in the viscous terms of the continuous kinetic energy equation (Eq. (4)).

Note that the dissipation is strictly negative definite only if the vorticity in the diffusion term is evaluated implicitly with $\omega_{\mathrm{n}} = \omega_{\mathrm{n}}^{n+1/2}$. This is often advisable for stability reasons anyway.

2.2.6. Summary. It has been shown that in two dimensions an unstructured staggered mesh discretization of the rotational form of the Navier–Stokes equations can satisfy the following equation:

$$\sum^{\text{cells}} V_{\mathrm{c}} \frac{K^{n+1} - K^n}{\Delta t} + \sum^{\substack{\text{bound}\\ \text{faces}}} \left(\frac{1}{2} \mathbf{u} \cdot \mathbf{u} \right)_{\mathrm{f}} \hat{u}^{n+1/2} A_{\mathrm{f}}$$
$$= \sum^{\substack{\text{bound}\\ \text{faces}}} p_{\mathrm{f}} \hat{u}^{n+1/2} A_{\mathrm{f}} + \sum^{\substack{\text{bound}\\ \text{faces}}} A_{\mathrm{f}} \frac{1}{2} \mathbf{t}_{\mathrm{f}} \cdot \sum^{\substack{\text{faces}\\ \text{nodes}}} \nu_{\mathrm{n}} \omega_{\mathrm{n}} \mathbf{u}_{\mathrm{n}} - \sum^{\text{nodes}} A_{\mathrm{n}} \nu_{\mathrm{n}} \omega_{\mathrm{n}} \omega_{\mathrm{n}}^{n+1/2}, \tag{29}$$

where the discrete kinetic energy is given by

$$K = \frac{1}{v_{\mathrm{c}}} \sum^{\substack{\text{cell}\\ \text{faces}}} W_{\mathrm{f}}^{\mathrm{c}} A_{\mathrm{f}} \left(\frac{1}{2} u u \right). \tag{30}$$

This is a discrete analog of the continuous kinetic energy transport equation. It is conservative in the absence of viscosity and purely dissipative in the presence of viscosity, with no artificial dissipation.

One subtle assumption in the derivation was in the form of the convective term itself. The convective term was evaluated by constructing $\omega \times \mathbf{u}$ at the nodes and averaging that result to the faces. Other possibilities, such as averaging the vorticity and velocity to the faces first and then taking the cross product, have not been evaluated.

It is interesting to note that the definition of the discrete vorticity defines a new operator, ROT (The notation ROT is borrowed from Ref. [8], which uses it in a similar context.):

$$\omega_n A_n = \sum_{\substack{\text{node}\\ \text{faces}}} \hat{u} W_f + \text{B.C.s} = \mathbf{ROT}(u W_f) + \text{B.C.s.} \tag{31}$$

It turns out that $\mathbf{ROT} = \mathbf{CURL}^T$, so the rotational form of the viscous term in the momentum equation is a symmetric positive semidefinite operator. This makes it relatively easy to invert via iterative methods and suitable for implicit solution.

2.3. *Conservation of Vorticity: Rotational Form*

For the continuous Navier–Stokes equations, vorticity conservation is derived by taking the curl of the momentum equation. If we continue to consider an incompressible fluid then vorticity evolution is given by the equation

$$\frac{\partial \omega}{\partial t} + \nabla \times (\omega \times \mathbf{u}) = -\nabla \times \nabla \times (\nu\omega), \tag{32}$$

which can also be written as

$$\frac{\partial \omega}{\partial t} + \nabla \cdot (\omega \mathbf{u}) = \omega \cdot \nabla \mathbf{u} + \nabla^2(\nu\omega), \tag{33}$$

where ω is the vorticity. In two dimensions the first term on the right-hand side of Eq. (33) is zero and vorticity is a conserved variable. In an inviscid incompressible two-dimensional flow all the moments of vorticity are also conserved quantities. In three dimensions, Eq. (32) is the more useful viewpoint and it indicates that in three dimensions the circulation (integral of velocity around a closed loop) is a conserved quantity. However, we continue to focus on the two-dimensional case in this section.

To show discrete vorticity conservation we use a discrete curl operation, specifically the **ROT** operation defined previously. This is equivalent to a counterclockwise line integral around the faces of the dual control volume surrounding a node. This is specifically performed by dividing the momentum equation by the face area (so it becomes an approximation for the momentum equation integrated along the face length), multiplying by -1 if the face normal points clockwise with respect to the node in question, and finally summing over all the faces touching a specific node. The result is a proof of local vorticity conservation. Global conservation is then shown by proving that the fluxes at neighboring node control volumes cancel out everywhere in the interior of the domain, leaving only boundary contributions. Nicolaides shows an alternative method of proving vorticity conservation in Ref. [22]. Discrete conservation of vorticity at a single node starts with the following equation,

$$\begin{aligned} &\sum_{\substack{\text{node}\\ \text{faces}}} W_f \frac{u^{n+1} - u^n}{\Delta t} - \sum_{\substack{\text{node}\\ \text{faces}}} W_f \, \mathbf{AVG}(\omega_n v_n) \\ &\quad = -\sum_{\substack{\text{node}\\ \text{faces}}} \mathbf{GRAD}\left(p_c^d\right) - \sum_{\substack{\text{node}\\ \text{faces}}} (W_f / A_f) \, \mathbf{CURL}(\nu_n \omega_n), \end{aligned} \tag{34}$$

where the normal vector at each face has been chosen to point in a direction counterclockwise with respect to the node in question. The goal is to recast this equation into a discrete analog

of the continuous vorticity transport equation given by Eq. (33). For the time being it will be assumed that the node or nodes in question are in the interior of the domain. Boundary nodes will be treated in Section 2.3.2.

2.3.1. Local vorticity conservation. If the node is an interior node then the sum over all node faces represents a closed line integral around the node, and the time derivative becomes an approximation for the change in vorticity at the node times the node area:

$$\sum^{\substack{\text{node}\\\text{faces}}} W_{\text{f}} \frac{u^{n+1}-u^n}{\Delta t} = A_{\text{n}} \frac{\omega_{\text{n}}^{n+1}-\omega_{\text{n}}^n}{\Delta t}. \tag{35}$$

The convection term can be expanded as follows,

$$\sum^{\substack{\text{node}\\\text{faces}}} W_{\text{f}}\, \mathbf{AVG}(v_{\text{n}}\omega_{\text{n}}) = \sum^{\substack{\text{node}\\\text{faces}}} (W_{\text{f}}/A_{\text{f}})[(\mathbf{x}_{\text{f}}^* - \mathbf{x}_{\text{n0}})\cdot \mathbf{v}_{\text{n0}}\omega_{\text{n0}} - (\mathbf{x}_{\text{f}}^* - \mathbf{x}_{\text{ni}})\cdot \mathbf{v}_{\text{ni}}\omega_{\text{ni}}], \tag{36}$$

where node n0 is the node over which summation is occurring and the face normal vector is assumed to point counterclockwise with respect to node n0. The node ni is a neighboring node to n0 connected by the face in question. This can be rewritten in the simpler form,

$$= \sum^{\substack{\text{node}\\\text{faces}}} W_{\text{f}} \frac{1}{2}[v_{\text{fn0}}\omega_{\text{n0}} + v_{\text{fni}}\omega_{\text{ni}}], \tag{37}$$

where v_{fn} is the velocity along the line pointing from the face to the node and outward. Each face contribution represents an approximation for the flux of vorticity into the node dual control volume (Voronoi cell). For uniform meshes, the velocity component is exactly perpendicular to the dual control volume faces. For nonuniform meshes the velocity is not exactly perpendicular, but the two tangential velocity components nearly cancel and the approximation is still a first-order approximation for the normal flux at the face.

The curl of a gradient is zero for continuous differential operators. The same is also true of the discrete unstructured staggered mesh operators, so the discrete curl operation also eliminates the pressure term in this discrete vorticity equation:

$$-\sum^{\substack{\text{node}\\\text{faces}}} \mathbf{GRAD}\left(p_{\text{c}}^{\text{d}}\right) = \sum^{\substack{\text{node}\\\text{faces}}} \left(p_{\text{c1}}^{\text{d}} - p_{\text{c2}}^{\text{d}}\right) = 0. \tag{38}$$

The cancellation occurs only if the faces completely surround the node, so this is not true for boundary nodes unless boundary conditions are introduced.

Finally, the viscous term becomes

$$\begin{aligned} -\sum^{\substack{\text{node}\\\text{faces}}} \mathbf{CURL}(\nu_{\text{n}}\omega_{\text{n}})W_{\text{f}}/A_{\text{f}} &= -\mathbf{ROT}[(W_{\text{f}}/A_{\text{f}})\,\mathbf{CURL}(\nu_{\text{n}}\omega_{\text{n}})] \\ &= \sum^{\substack{\text{node}\\\text{faces}}} (\nu_{\text{ni}}\omega_{\text{ni}} - \nu_{\text{n0}}\omega_{\text{n0}})W_{\text{f}}/A_{\text{f}}, \end{aligned} \tag{39}$$

which is a symmetric, negative semidefinite, conservation diffusion term.

The final equation becomes

$$A_{\text{n}}\frac{\omega^{n+1}-\omega^n}{\Delta t} + \sum^{\substack{\text{node}\\\text{faces}}} \left(\left(\frac{1}{2}\{v_{\text{nf0}}\omega_{\text{n0}} + v_{\text{nfi}}\omega_{\text{ni}}\}\right) = \sum^{\substack{\text{node}\\\text{faces}}} (\nu_{\text{ni}}\omega_{\text{ni}} - \nu_{\text{n0}}\omega_{\text{n0}})W_{\text{f}}/A_{\text{f}}, \right. \tag{40}$$

where the convection velocity at each face is given by $v_{\mathrm{nf}} = (\mathbf{x}_{\mathrm{f}}^{*} - \mathbf{x}_{\mathrm{ni}}) \cdot \mathbf{v}_{\mathrm{ni}} 2/A_{\mathrm{f}}$. Note that Eq. (40) can be interpreted as a control volume discretization of the vorticity equation integrated over the dual mesh control volumes (Voronoi cells) surrounding each node.

2.3.2. Global vorticity conservation. Global conservation is a direct consequence of the fact that the convective and diffusive vorticity fluxes at interior faces are equal and opposite for the two nodes touching each face. Consequently, the contributions from all interior faces cancel out.

However, to rigorously account for all the vorticity in the domain it is necessary to include the vorticity contributions from boundary nodes and their associated dual control volumes. In order to account correctly for the vorticity at boundary nodes, the dual control volumes must be closed by connecting the centers of the two boundary faces touching each boundary node. If boundary conditions are used to define appropriate approximations to the momentum equation along this new dual control volume face, then the analysis of Section 2.3.1 above remains valid.

When global conservation is analyzed by summing over the area weighted vorticity from all nodes in the domain, including boundary nodes, the fluxes from the new dual control volume faces at the boundaries do not cancel. The result is that the net change in total vorticity is due to the vorticity fluxes through these dual control volume faces at the boundaries.

3. ANALYSIS OF THE DIVERGENCE FORM

The next discretization that will be considered is based on the well known divergence form of the Navier–Stokes equations:

$$\frac{\partial \mathbf{u}}{\partial t} + \nabla \cdot (\mathbf{u}\mathbf{u}) = -\nabla p + \nabla \cdot \nu(\nabla \mathbf{u} + \nabla \mathbf{u}^{\mathrm{T}}). \tag{41}$$

Discretizations based on the divergence form of the equations are of interest because they are expected to be able to discretely conserve linear momentum. Note that conservation of momentum is by no means guaranteed by using this form, because the staggered mesh methods update only the normal velocity components at cell faces; tangential velocity components are interpolated. The primary disadvantage of the divergence form is that in the context of unstructured staggered mesh methods the divergence form requires more computational and memory overhead.

3.1. *Unstructured Discretization of the Divergence Form*

At interior faces the orientation of the normal is chosen to point from cell C1 to cell C2, at boundary faces the normal vector is assumed to point out of the domain. The discrete equation for the evolution of the normal velocity component is given by

$$W_{\mathrm{f}} A_{\mathrm{f}} \frac{u^{n+1} - u^{n}}{\Delta t} \mathbf{n}_{\mathrm{f}} \cdot \left(W_{\mathrm{C1}}^{\mathrm{f}} \mathbf{c}_{\mathrm{c1}} + W_{\mathrm{C2}}^{\mathrm{f}} \mathbf{c}_{\mathrm{c2}} \right) A_{\mathrm{f}} = -(p_{\mathrm{c2}} - p_{\mathrm{c1}}) A_{\mathrm{f}} + \mathbf{n}_{\mathrm{f}} \cdot \left(W_{\mathrm{C1}}^{\mathrm{f}} \mathbf{d}_{\mathrm{c1}} + W_{\mathrm{C2}}^{\mathrm{f}} \mathbf{d}_{\mathrm{c2}} \right) A_{\mathrm{f}}, \tag{42}$$

where $\mathbf{c}_{\mathrm{c}} = \frac{1}{v_{\mathrm{c}}} \sum^{\text{cell faces}} \mathbf{u}_{\mathrm{f}} \hat{u} A_{\mathrm{f}}$ is a conservative discretization of the convection term evaluated in each cell, $\mathbf{d}_{\mathrm{c}} = \frac{1}{v_{\mathrm{c}}} \sum^{\text{cell faces}} \nu(\nabla \mathbf{u} + \nabla \mathbf{u}^{\mathrm{T}}) \cdot \hat{\mathbf{n}}_{\mathrm{f}} A_{\mathrm{f}}$ is a conservative discretization of the diffusion term evaluated in each cell, V_{c} is the volume of each cell (which is really an area

times unit depth), and W_C^f is the distance between the face circumcenter and the cell circumcenter. Remember that $u = \mathbf{u} \cdot \mathbf{n}_f$ is the normal velocity at each cell face and $\hat{u}$ is the normal velocity component that points out of the cell. This discretization continues to assume that the mesh cells have a unique circumcenter, so that the face normal continues to point directly away from one cell center and directly toward another cell center. The following analysis will indicate that specific interpolations for the face velocity, $\mathbf{u}_f$, and velocity gradient at the cell faces, $\nabla\mathbf{u}$, are necessary in order to conserve discrete kinetic energy.

3.2. *Conservation of Kinetic Energy: Divergence Form*

The proof of discrete kinetic energy conservation of the divergence form begins just like the proof for the rotational form. Each equation for the normal velocity at the face is multiplied by the half-time normal velocity, $u^{n+1/2}$, and then summed over the faces. Discrete conservation of kinetic energy is derived by showing that a discrete form of integration by parts can be applied to each term of the normal momentum equation. Then it is shown that this portion of the kinetic energy (that due to the normal velocity summed over all cell faces) is an approximation for the full kinetic energy within each mesh cell.

Discrete kinetic energy conservation of the divergence form starts with the following equation:

$$\sum^{\text{faces}} u^{n+1/2} W_f A_f \frac{u^{n+1} - u^n}{\Delta t} + \sum^{\text{faces}} u^{n+1/2} \mathbf{n}_f \cdot \left(W_{C1}^f \mathbf{c}_{c1} + W_{C2}^f \mathbf{c}_{c2} \right) A_f$$
$$= - \sum^{\text{faces}} u^{n+1/2} A_f \, \mathbf{GRAD}(p_c) + \sum^{\text{faces}} u^{n+1/2} \mathbf{n}_f \cdot \left(W_{C1}^f \mathbf{d}_{c1} + W_{C2}^f \mathbf{d}_{c2} \right) A_f. \quad (43)$$

The time derivative remains the same as in the standard rotational discretization (Section 2.2.1) and will not be reevaluated. The pressure gradient term has also been analyzed in the context of the standard rotational discretization (Section 2.2.4); the only difference is that in this context the pressure gradient term contains only the pressure, not the dynamic pressure. The following analysis will therefore focus on the convection and diffusion terms.

3.2.1. Convection term. The convection term can be rewritten as a summation over cells,

$$\sum^{\text{faces}} u^{n+1/2} \mathbf{n}_f \cdot \left(W_{C1}^f \mathbf{c}_{c1} + W_{C2}^f \mathbf{c}_{c2} \right) A_f = \sum^{\text{cells}} \mathbf{c}_c \cdot \sum^{\substack{\text{cell} \\ \text{faces}}} u^{n+1/2} \mathbf{n}_f W_C^f A_f = \sum^{\text{cells}} \mathbf{c}_c \cdot \mathbf{u}_c^* V_c, \quad (44)$$

where $\mathbf{u}_c^* = \frac{1}{v_c} \sum^{\text{cell faces}} u^{n+1/2} \mathbf{n}_f W_C^f A_f$ is an approximation for the velocity vector in the cells. Section 5.4 proves that this is a first-order approximation for the velocity vector.

Expanding the convection vector, $\mathbf{c}$, it is found that Eq. (44) becomes

$$= \sum^{\text{cells}} \mathbf{u}_C^* \cdot \sum^{\substack{\text{cell} \\ \text{faces}}} \mathbf{u}_f \hat{u} A_f = \sum^{\substack{\text{interior} \\ \text{faces}}} (\mathbf{u}_{c1}^* - \mathbf{u}_{c2}^*) \cdot \mathbf{u}_f (u A_f) + \sum^{\substack{\text{boundary} \\ \text{faces}}} \mathbf{u}_{c1}^* \cdot \mathbf{u}_f (\hat{u} A_f). \quad (45)$$

If the face velocity $\mathbf{u}_f$ at interior faces is required to be a simple average of $\mathbf{u}_c^*$ from the

neighboring cells then

$$= \sum_{\text{faces}}^{\text{interior}} (\mathbf{u}^*_{c1} - \mathbf{u}^*_{c2}) \cdot \frac{1}{2}(\mathbf{u}^*_{c1} + \mathbf{u}^*_{c2})(uA_f) + \sum_{\text{faces}}^{\text{boundary}} \mathbf{u}^*_{c1} \cdot \mathbf{u}_f(\hat{u}A_f) \quad (46)$$

$$= \sum_{\text{faces}}^{\text{interior}} \frac{1}{2}\left[(\mathbf{u}^*_{c1})^2 - (\mathbf{u}^*_{c2})^2\right](uA_f) + \sum_{\text{faces}}^{\text{boundary}} \mathbf{u}^*_{c1} \cdot \left[\left\{\mathbf{u}_f - \frac{1}{2}\mathbf{u}^*_{c1}\right\} + \frac{1}{2}\mathbf{u}^*_{c1}\right](\hat{u}A_f). \quad (47)$$

This can be converted back into a summation over cells which then disappears due to the continuity constraint,

$$= \sum^{\text{cells}} \frac{1}{2}(\mathbf{u}^*_c)^2 \sum_{\text{faces}}^{\text{cells}} uA_f + \sum_{\text{faces}}^{\text{boundary}} \mathbf{u}^*_{cl} \cdot \left[\mathbf{u}_f - \frac{1}{2}\mathbf{u}^*_{c1}\right](\hat{u}A_f) = \sum_{\text{faces}}^{\text{boundary}} \left[\frac{1}{2}\mathbf{u}^*_{c1} \cdot \mathbf{u}^*_E\right](\hat{u}A_f), \quad (48)$$

where $\mathbf{u}^*_E = 2\mathbf{u}_f - \mathbf{u}^*_{c1}$ is an extrapolated velocity at the boundary faces, resulting in a second-order approximation for the kinetic energy at the boundary faces. The result indicates that kinetic energy fluxes cancel out on the interior faces, and the only net convection of kinetic energy occurs through the boundaries.

3.2.2. Diffusive term. The diffusive term can also be written as a summation over cells:

$$\sum^{\text{faces}} u^{n+1/2}\mathbf{n}_f \cdot \left(W^f_{C1}\mathbf{d}_{c1} + W^f_{C2}\mathbf{d}_{c2}\right)A_f = \sum^{\text{cells}} \mathbf{d}_c \cdot \sum_{\text{faces}}^{\text{cell}} u^{n+1/2}\mathbf{n}_f W^f_C A_f = \sum^{\text{cells}} \mathbf{d}_c \cdot \mathbf{u}^*_c V_c. \quad (49)$$

For simplicity we assume constant viscosity and incompressible flow. Then expanding the diffusion vector, $\mathbf{d}$, it is found that this expression becomes,

$$= \sum^{\text{cells}} \mathbf{u}^*_c \cdot \sum_{\text{faces}}^{\text{cell}} \nu \frac{\partial \mathbf{u}}{\partial \hat{n}} A_f = \sum^{\text{faces}} (\mathbf{u}^*_{c1} - \mathbf{u}^*_{c2}) \cdot \left[\nu \frac{\partial \mathbf{u}}{\partial n}\right] A_f + \sum_{\text{faces}}^{\text{boundary}} [\mathbf{u}^*_{c2}] \cdot \left[\nu \frac{\partial \mathbf{u}}{\partial n}\right] A_f, \quad (50)$$

where $\mathbf{u}^*_{c2}$ equals the face velocity on boundary faces. This is equivalent to

$$= -\sum^{\text{faces}} \frac{\partial \mathbf{u}^*_c}{\partial n} \cdot \nu \frac{\partial \mathbf{u}}{\partial n} A_f W_f + \sum_{\text{faces}}^{\text{boundary}} \mathbf{u}_f \cdot \left[\nu \frac{\partial \mathbf{u}}{\partial \hat{n}}\right] A_f. \quad (51)$$

The first term is a discrete approximation for the dissipation rate. If the velocity gradient at the faces is evaluated using $\mathbf{u}^*_c$ then the dissipation is a negative semidefinite quantity. The second term is the viscous work term at the boundaries of the domain.

3.2.3. Summary. It has been shown that for constant viscosity, the two-dimensional divergence form of the unstructured staggered mesh scheme satisfies the following discrete kinetic energy equation,

$$\sum^{\text{cells}} V_c \frac{K^{n+1} - K^n}{\Delta t} + \sum_{\text{faces}}^{\text{boundary}} \left[\frac{1}{2}\mathbf{u}^*_{c1} \cdot \mathbf{u}^*_E\right](\hat{u}A_f)$$
$$= \sum_{\text{faces}}^{\text{boundary}} p_f \hat{u}^{n+1/2} A_f + \sum_{\text{faces}}^{\text{boundary}} \mathbf{u}_f \cdot \left[\nu \frac{\partial \mathbf{u}}{\partial \hat{n}}\right] A_f - \sum^{\text{cells}} V_c \varepsilon_c, \quad (52)$$

where the discrete kinetic energy is given by

$$K = \frac{1}{V_c} \sum^{\substack{\text{cell} \\ \text{faces}}} W_f^C A_f \left(\frac{1}{2} uu \right), \tag{53}$$

and the discrete dissipation is given by

$$\varepsilon_c = \frac{1}{V_c} \sum^{\substack{\text{cell} \\ \text{faces}}} \frac{\partial \mathbf{u}_c^*}{\partial n} \cdot \nu \frac{\partial \mathbf{u}}{\partial n} A_f W_f^C. \tag{54}$$

The construction of the discrete kinetic energy evolution equation required that cell velocity and face velocity interpolations were based on

$$\mathbf{u}_c^* = \frac{1}{\nu_c} \sum^{\substack{\text{cell} \\ \text{faces}}} u^{n+1/2} \mathbf{n}_f W_C^f A_f, \tag{55}$$

which is a first-order accurate approximation of the cell velocity for arbitrary two-dimensional meshes.

3.3. *Conservation of Momentum: Divergence Form*

For standard control volume discretizations, momentum conservation is a straightforward consequence of writing the equations in divergence form. However, a proof of conservation of momentum is far less obvious for staggered mesh numerical schemes on unstructured meshes. The inherent difficulty is due to the fact that the velocity vector is not a uniquely defined quantity in such methods. Part of the proof of momentum conservation will be to derive how the velocity vector should best be defined.

To show discrete momentum conservation we multiply each equation for the normal velocity at the face by the face normal vector, and sum over the faces. Initially, this appears to be an incomplete procedure since only a portion of the momentum at each face is being analyzed. However, it will be shown that this can be reinterpreted as evolution equation for the velocity vector in each cell, and this evolution equation is conservative.

If the summation is performed over all the faces of a single control volume then the following proof is a statement of local momentum conservation. It states that the change in momentum within the control volume is only a result of fluxes through the control volume surfaces. If the summation is performed over all the faces in a mesh (including the boundary faces) then the interior fluxes cancel out and the resulting proof is a statement of global conservation. Global conservation states that the change in momentum is due only to fluxes through the boundary of the domain.

Discrete momentum conservation of the divergence form starts with the following equation:

$$\begin{aligned} &\sum^{\text{faces}} \mathbf{n}_f W_f A_f \frac{u^{n+1} - u^n}{\Delta t} + \sum^{\text{faces}} \mathbf{n}_f \mathbf{n}_f \cdot \left(W_{C1}^f \mathbf{c}_{c1} + W_{C2}^f \mathbf{c}_{c2} \right) A_f \\ &\quad = - \sum^{\text{faces}} \mathbf{n}_f A_f \, \mathbf{GRAD}(p_c) + \sum^{\text{faces}} \mathbf{n}_f \mathbf{n}_f \cdot \left(W_{C1}^f \mathbf{d}_{c1} + W_{C2}^f \mathbf{d}_{c2} \right) A_f. \end{aligned} \tag{56}$$

The goal will be to recast this equation as an equation for the cell velocity vector. Critical

to this transformation is the definition of the cell velocity vector in terms of the face normal velocity components. Each term in this equation is evaluated below.

3.3.1. Time derivative. Remember that the width W_f is the distance between the neighboring two cell circumcenters (Fig. 2). On boundary faces, W_f is the distance from the interior cell circumcenter to the face circumcenter. The width can be decomposed into two parts, each representing the distance from the face circumcenter to one of the cell circumcenters. $W_f = W_f^{C1} + W_f^{C2}$. On boundary faces the second part is zero. With this notation, the sum over faces can be recast as summation over the cells,

$$\sum^{\text{faces}} W_f A_f \mathbf{n}_f \frac{u^{n+1} - u^n}{\Delta t} = \sum^{\text{faces}} \left(W_f^{C1} + W_f^{C2}\right) A_f \frac{\mathbf{n}_f u^{n+1} - \mathbf{n}_f u^n}{\Delta t} = \sum^{\text{cells}} \left[\sum^{\substack{\text{cell}\\ \text{faces}}} W_f^C A_f \frac{\mathbf{n}_f u^{n+1} - \mathbf{n}_f u^n}{\Delta t} \right], \tag{57}$$

where the term in square brackets can be identified as the change in the velocity vector within the cell. The velocity vector in a cell is therefore defined by the first-order approximation,

$$\mathbf{u}_c = \frac{1}{V_c} \sum^{\substack{\text{cell}\\ \text{faces}}} W_f^C A_f \mathbf{n}_f u, \tag{58}$$

where V_c is the volume of the cell. With the cell velocity vector defined in this way, the time derivative term can be written as

$$= \sum^{\text{cells}} V_c \frac{\mathbf{u}_c^{n+1} - \mathbf{u}_c^n}{\Delta t}. \tag{59}$$

This equation is valid for a collection of cells or an individual mesh cell.

3.3.2. Convection term. The convection term can be rewritten as a summation over cells:

$$\sum^{\text{faces}} \mathbf{n}_f \mathbf{n}_f \cdot \left(W_{C1}^f \mathbf{c}_{c1} + W_{C2}^f \mathbf{c}_{c2}\right) A_f = \sum^{\text{cells}} \mathbf{c}_c \cdot \left[\sum^{\substack{\text{cell}\\ \text{faces}}} \mathbf{n}_f \mathbf{n}_f W_C^f A_f \right] = \sum^{\text{cells}} \mathbf{c}_c \cdot \mathbf{I} V_c = \sum^{\text{cells}} \mathbf{c}_c V_c. \tag{60}$$

The term in brackets is equal to the identity tensor $\mathbf{I}$, times the cell volume. This is a known geometric identity, but the user can prove it using the basic techniques described in Section 5. We can now expand the convection term using its definition,

$$= \sum^{\text{cells}} \sum^{\substack{\text{cell}\\ \text{faces}}} \mathbf{u}_f \hat{u} A_f = \sum^{\substack{\text{boundary}\\ \text{faces}}} \mathbf{u}_f \hat{u} A_f. \tag{61}$$

There are two contributions from each interior face, and they exactly cancel out, since $\hat{u}$ is equal and opposite for the two contributions. The remaining term is the flux of momentum into the domain, across the boundary faces.

3.3.3. Pressure gradient term. The gradient term in the kinetic energy can be rearranged as

$$-\sum^{\text{faces}} \mathbf{n}_\text{f} A_\text{f}\, \mathbf{GRAD}(p_\text{c}) = -\sum^{\text{faces}} \mathbf{n}_\text{f} A_\text{f}(p_{\text{c}2} - p_{\text{c}1}) = \sum^{\text{cells}} p_\text{c} \sum^{\substack{\text{cell}\\ \text{faces}}} \hat{\mathbf{n}}_\text{f} A_\text{f}$$
$$- \sum^{\substack{\text{boundary}\\ \text{faces}}} p_{\text{c}2}\hat{\mathbf{n}}_\text{f} A_\text{f} = - \sum^{\substack{\text{boundary}\\ \text{faces}}} p_\text{f}\hat{\mathbf{n}}_\text{f} A_\text{f}, \tag{62}$$

where $\hat{\mathbf{n}}_\text{f}$ is the normal vector pointing out of the cell, or in the case of boundary faces—out of the domain.

3.3.4. Diffusion term. The diffusion term behaves very similarly to convection,

$$\sum^{\text{faces}} \mathbf{n}_\text{f}\mathbf{n}_\text{f} \cdot \left(W^\text{f}_{\text{C}1}\mathbf{d}_{\text{c}1} + W^\text{f}_{\text{c}2}\mathbf{d}_{\text{c}2}\right) A_\text{f} = \sum^{\text{cells}} \mathbf{d}_\text{c} \cdot \left[\sum^{\substack{\text{cell}\\ \text{faces}}} \mathbf{n}_\text{f}\mathbf{n}_\text{f} W^\text{f}_\text{C} A_\text{f}\right] = \sum^{\text{cells}} \mathbf{d}_\text{c} \cdot \mathbf{I} V_\text{c} = \sum^{\text{cells}} \mathbf{d}_\text{c} V, \tag{63}$$

where the bracketed term can be replaced by the identity matrix for two-dimensional meshes. Expanding the diffusion vector, $\mathbf{d}$, it is found that

$$\sum^{\text{cells}} \sum^{\substack{\text{cell}\\ \text{faces}}} \nu(\nabla\mathbf{u} + \nabla\mathbf{u}^\text{T})_\text{f} \cdot \hat{\mathbf{n}}_\text{f} A_\text{f} = \sum^{\substack{\text{boundary}\\ \text{faces}}} \nu(\nabla\mathbf{u} + \nabla\mathbf{u}^\text{T})_\text{f} \cdot \hat{\mathbf{n}}_\text{f} A_\text{f}. \tag{64}$$

Again, there are two contributions from each interior face, and they exactly cancel out, since $\hat{\mathbf{n}}_\text{f}$ is equal and opposite for the two contributions, and all other quantities are identical. The remaining term is the viscous flux of momentum into the domain, across the boundary faces.

Note that the rotational form of the viscous term also conserves momentum. The rotational form is

$$-\sum^{\text{faces}} \mathbf{n}_\text{f} W_\text{f}\, \mathbf{CURL}(\nu_\text{n}\omega_\text{n}) = \sum^{\text{faces}} \mathbf{n}_\text{f} W_\text{f} \sum^{\substack{\text{face}\\ \text{nodes}}} \nu_\text{n}\hat{\omega}_\text{n} = \sum^{\text{nodes}} \nu_\text{n}\omega_\text{n} \sum^{\substack{\text{node}\\ \text{faces}}} \hat{\mathbf{n}}_\text{f} W_\text{f}. \tag{65}$$

On interior nodes the last summation is zero. On boundary nodes the summation over node faces is simply the difference between the neighboring two boundary face circumcenters, so we obtain

$$= \sum^{\substack{\text{boundary}\\ \text{nodes}}} \nu_\text{n}\omega_\text{n}\left(\mathbf{x}^{\text{CC}}_{\text{f}2} - \mathbf{x}^{\text{CC}}_{\text{f}1}\right) = \sum^{\substack{\text{boundary}\\ \text{faces}}} \mathbf{x}^{\text{CC}}_\text{f} \sum^{\substack{\text{face}\\ \text{nodes}}} \nu_\text{n}\hat{\omega}_\text{n}. \tag{66}$$

The summation over face nodes is a discrete approximation for the normal component of the diffusive term integrated over each boundary face. The entire summation is a first-order approximation for the total diffusion of velocity within the domain. While this is not the classic divergence form of the diffusion term this representation is equally valid and conservative.

3.3.5. Summary. It has been shown that the divergence form of the unstructured staggered mesh scheme satisfies the following first-order conservative equation for the evolution

of the cell velocities (or momentum),

$$\sum^{\text{cells}} V_c \frac{\mathbf{u}_c^{n+1} - \mathbf{u}_c^n}{\Delta t} + \sum^{\substack{\text{boundary}\\ \text{faces}}} \mathbf{u}_f \hat{u} A_f = - \sum^{\substack{\text{boundary}\\ \text{faces}}} p_f \hat{\mathbf{n}}_f A_f + \sum^{\substack{\text{boundary}\\ \text{faces}}} \nu(\nabla \mathbf{u} + \nabla \mathbf{u}^T)_f \cdot \hat{\mathbf{n}}_f A_f, \quad (67)$$

where the cell velocity is given by the first-order approximation

$$\mathbf{u}_c = \frac{1}{V_c} \sum^{\substack{\text{cell}\\ \text{faces}}} W_f^C A_f \mathbf{n}_f u. \quad (68)$$

This indicates that the unstructured staggered mesh discretization of the divergence form of the Navier–Stokes equations is fully equivalent to a control volume method for the velocity vector located at cell centers.

4. NUMERICAL TESTS OF CONSERVATION

In order to test the conservation properties of these schemes a problem was chosen that has zero mass flux at the boundaries, but is inherently unsteady. The problem involves a roughly circular patch of constant vorticity (magnitude of 2 s^{-1}) located in the bottom left quadrant of a square domain. The domain boundaries are slip walls. The vortex patch is 10 cm in diameter and the square domain is 100 cm. The vortex rotates counterclockwise with a maximum speed of 6 cm/s, and its center moves counterclockwise around the domain at a speed of roughly 0.5 cm/s. A total of 6200 triangles are used to spatially discretize the domain. The initial streamlines are shown in Fig. 3a. The mesh and the initial vortex patch are shown in Fig. 3b.

4.1. *Conservation of Kinetic Energy*

The discrete kinetic energy within each mesh cell was calculated at every time step using Eq. (8). The average discrete kinetic energy was then evaluated by calculating the volume weighted sum over all the cell kinetic energies, $\text{KE}_{\text{average}} = \frac{1}{V_{\text{domain}}} \sum^{\text{cells}} V_c K_c$. Since there is no flow across the domain boundaries, this quantity should be constant in the absence of viscosity, and monotonically decreasing in the presence of viscosity with a decay rate proportional to the viscosity times the enstrophy.

In numerical tests of the vortex motion in the absence of viscosity, the average discrete kinetic remained constant to six significant digits after 200 time steps (10 s). This is about as constant as can be expected given the tolerances prescribed for the iterative solver. This level of accuracy was achieved for both the divergence and rotational discretizations. Figure 4a shows the change in the average discrete kinetic energy as a function of time when viscosity is present (0.1 and 0.001 cm^2/s). Both the rotational (dashed lines) and the divergence forms (solid lines) are shown. The lower two curves are the higher viscosity case. In both cases, the divergence form tends to dissipate more kinetic energy than the rotational form in the early stages of the evolution. It is hypothesized that this is because the divergence form contains two extra averaging operations as compared to the rotational form. Since the vorticity is initially discontinuous, these extra averaging operations introduce artificial dissipation in the early stages of the vortex evolution. After roughly one diffusion time scale the vorticity becomes smoother and the two methods dissipate at nearly equal rates, as seen for the higher viscosity case.

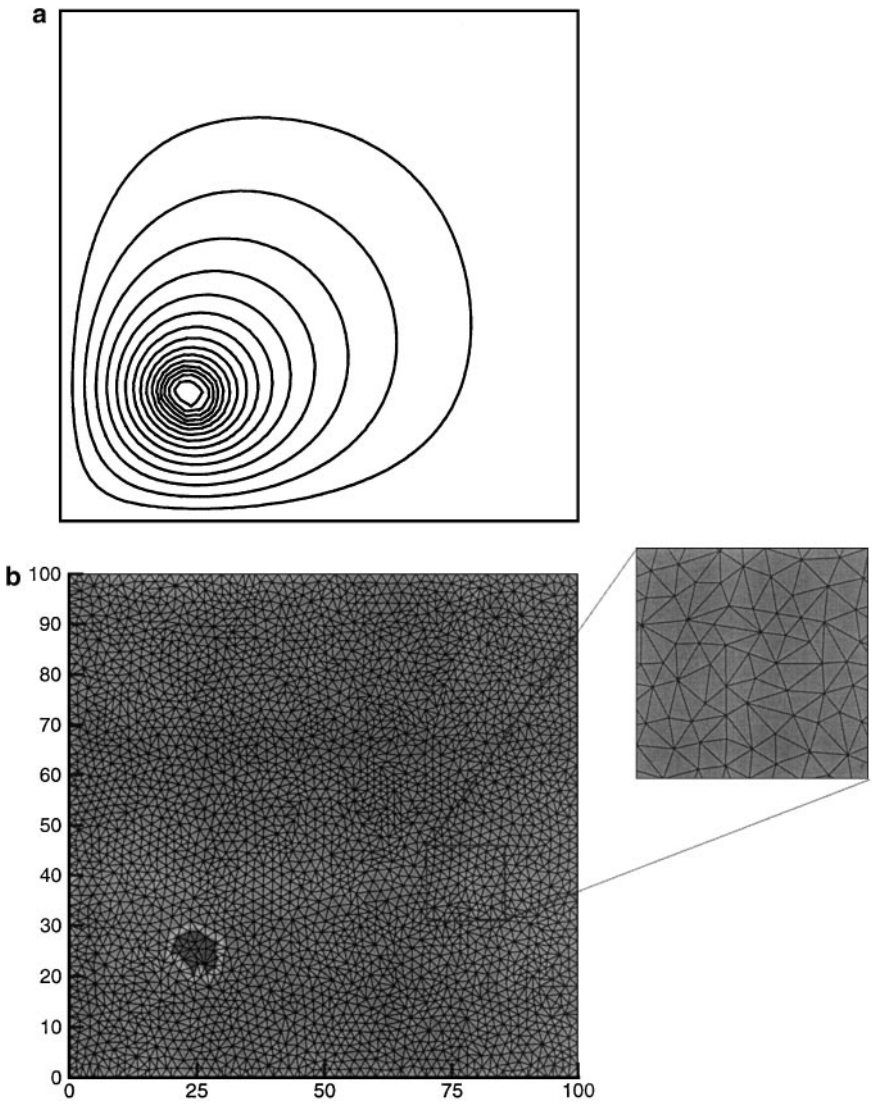

FIG. 3. (a) Initial streamlines for the off-center vortex in a box. (b) Initial vorticity and mesh.

The dissipation rate (time derivative of kinetic energy) for the rotational discretization is examined in more detail in Fig. 4b. This figure shows the previous two viscosity values and the actual derivative of kinetic energy (lines) compared to the average discrete dissipation rate theoretically determined in the text ($\frac{1}{V_{\text{domain}}} \sum^{\text{nodes}} \nu \omega_{\text{n}}^2 A_{\text{n}}$) which is represented by symbols. The match between symbols and lines indicates that the theoretical analysis of Section 2.2 is well founded.

4.2. *Conservation of Vorticity*

The discrete vorticity within each mesh cell was calculated at every time step using Eq. (26). The average discrete vorticity was then evaluated by calculating the area weighted sum over all the individual node vorticity values, $\Omega_{\text{average}} = \frac{1}{A_{\text{domain}}} \sum^{\text{nodes}} A_{\text{n}} \omega_{\text{n}}$. Since there

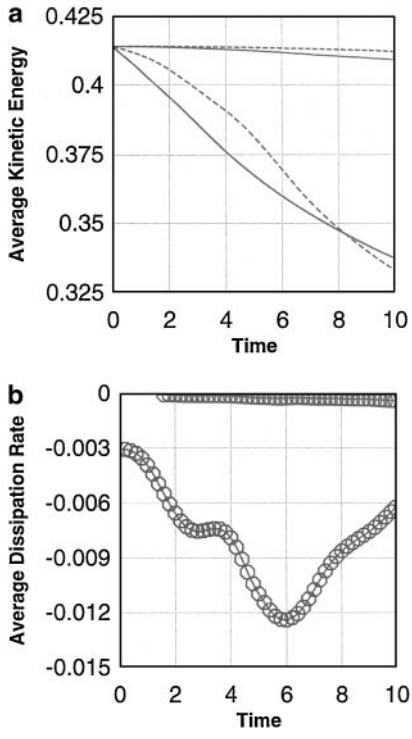

FIG. 4. (a) Kinetic energy as a function of time with kinematic viscosity of 0.1 and 0.001 cm^2/s. Solid lines are the divergence discretization and dashed lines are the rotational discretization. (b) Dissipation rate (time derivative of kinetic energy) as a function of time for the rotational form at two different values of the kinematic viscosity (0.1 and 0.001 cm^2/s). Solid lines are the actual time derivative, and open circles are the calculated discrete dissipation rate (viscosity times discrete vorticity squared).

is no flow across the domain boundaries, and the diffusive vorticity flux is zero at the domain boundaries, this quantity should be constant, even in the presence of viscosity.

Figure 5 shows the change in the average vorticity as a function of time, for two different values of the viscosity (0.1 and 0.001 cm^2/s) and both the rotational and divergence discretizations. The rotational form (dashed lines) conserves vorticity to seven significant

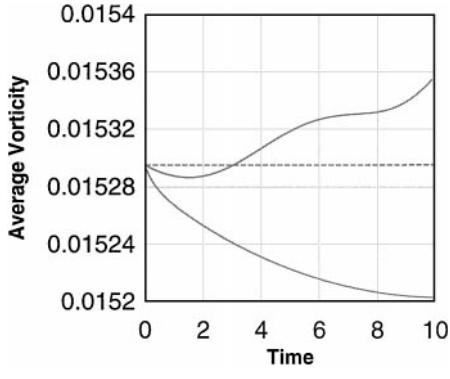

FIG. 5. Average vorticity as a function of time for two different values of the viscosity. The solid lines are the divergence discretization, and dashed lines are the rotational discretization. The lower curve is the higher viscosity case.

figures after the solution has evolved for 10 s (200 time steps). The divergence form (solid lines) does not conserve vorticity.

Theoretically, the total enstrophy (vorticity squared) is conserved in the absence of viscosity. However, this conservation property is not captured by either the rotational or the divergence discretization methods.

4.3. *Conservation of Momentum*

The discrete velocity (momentum) within each mesh cell was calculated at every time step using Eq. (55). The average discrete velocity was then evaluated by calculating the volume weighted sum over all the individual cell velocity values, $\mathbf{V}_{\text{average}} = \frac{1}{\text{V}_{\text{domain}}} \sum^{\text{cells}} V_{\text{c}} \mathbf{u}_{\text{c}}$. Since there is no flow across the domain boundaries, and because we are using slip walls, this quantity should remain constant even in the presence of viscosity.

It was found that both discretizations conserved the average x and y momentum to machine precision. The global conservation of momentum of the rotational discretization was not shown analytically in the text, but was determined to be a result of the fact that the streamfunction on the boundaries does not change with time.

A more difficult test of conservation was also performed by superimposing a uniform x velocity (5 cm/s) on the previous test problem and allowing the left boundary to be an inflow condition and the right boundary to be an outflow condition. This situation has a time varying streamfunction at the outflow. The divergence discretization continued to conserve x momentum to machine precision (y momentum is not constant for this problem).

5. ACCURACY OF STAGGERED MESH METHODS

In this section a new approach to determining the order of accuracy of unstructured staggered mesh discretizations is presented. This method as not based on Taylor series expansions which become unwieldy for two-dimensional unstructured meshes. Nor is it based on showing that the solution lies in a function space of piecewise polynomials of a certain order as is customary in finite element methods.

Instead it will be shown that discrete versions of Gauss' Divergence Theorem and Stokes Curl Theorem can be used to obtain estimates of accuracy. A number of the interpolations and approximations that are used in the analysis are not obviously first-order approximations. These interpolation methods are analyzed in more detail below.

5.1. *Rotational Convection Term*

This section looks at approximations for the convective term normal to the faces, $(\omega \times \mathbf{u}) \cdot \mathbf{n}_{\text{f}}$.

We begin with Stokes Theorem for an arbitrary bounded surface and a vector quantity $\mathbf{f}$,

$$\int_S (\nabla \times \mathbf{f}) \cdot \mathbf{n}\, dA = \int_{\partial \text{S}} \mathbf{f} \cdot \hat{\mathbf{z}}\, dL, \tag{69}$$

where S is a surface with normal $\mathbf{n}$, and ∂S is the boundary of the surface with unit tangential vector $\hat{\mathbf{z}}$ oriented in a counterclockwise direction around the boundary with respect to the face normal. In two dimensions, $\hat{\mathbf{z}}$ points into or out of the plane of interest.

The surfaces of interest in this case are the faces of the mesh which are actually line segments in two dimensions. The boundary of this surface is the two end points or nodes delimiting the line segment. So in two dimensions Stokes Theorem simplifies to

$$\mathbf{n}_\mathrm{f} \cdot \int_S (\nabla \times \mathbf{f})\, dA = \mathbf{z} \cdot (\mathbf{f}_{\mathrm{n}2} - \mathbf{f}_{\mathrm{n}1}), \tag{70}$$

where $\mathbf{z}$ is the vector which points out of the two-dimensional plane.

To analyze the convection term set $\mathbf{f} = (\mathbf{u} \cdot \mathbf{r})\omega$, where $\mathbf{r} = \mathbf{x} - \mathbf{x}_0$ is the position vector with an arbitrary origin $\mathbf{x}_0$. Then

$$\mathbf{n}_\mathrm{f} \cdot \int_S (\nabla \times (\mathbf{u} \cdot \mathbf{r})\omega)\, dA = \mathbf{z} \cdot [(\mathbf{u} \cdot \mathbf{r})\omega|_{\mathrm{n}2} - (\mathbf{u} \cdot \mathbf{r})\omega|_{\mathrm{n}1}] = (\mathbf{u} \cdot \mathbf{r}\omega_\mathrm{z})|_{\mathrm{n}2} - (\mathbf{u} \cdot \mathbf{r}\omega_\mathrm{z})|_{\mathrm{n}1}. \tag{71}$$

In Cartesian tensor notation the left-hand side of this equation is written as

$$n_i \int_S \varepsilon_{ijk}(u_\mathrm{s} r_\mathrm{s} \omega_\mathrm{k})_{,j}\, dA = n_i \int_S \varepsilon_{ijk}[u_\mathrm{s}\omega_\mathrm{k} r_{\mathrm{s},j} + r_\mathrm{s}(u_\mathrm{s}\omega_\mathrm{k})_{,j}]\, dA. \tag{72}$$

The gradient of the position vector is the identity matrix, ($r_{\mathrm{s},j} = \delta_{\mathrm{s}j}$). So we can now write that

$$-\mathbf{n}_\mathrm{f} \cdot \int_S \omega \times \mathbf{u}\, dA + n_i \int_S \varepsilon_{ijk} r_\mathrm{s}(u_\mathrm{s}\omega_\mathrm{k})_{,j}\, dA = (\mathbf{u} \cdot \mathbf{r}\omega_\mathrm{z})|_{\mathrm{n}2} - (\mathbf{u} \cdot \mathbf{r}\omega_\mathrm{z})|_{\mathrm{n}1}, \tag{73}$$

where ω_z is the vorticity at the node which points out of the 2D plane. Note that this is an exact equation. The second term cannot be simply written in vector notation so it has been left in Cartesian tensor notation.

This equation can be used to develop discrete approximations for the rotational convection term, $(\omega \times \mathbf{u})_\mathrm{f} \cdot \mathbf{n}_\mathrm{f}$. Assume that the velocity field $\mathbf{u}$ and the vorticity field ω are constant along the face so that $\omega \times \mathbf{u}$ is a constant vector on the face. This is a first-order approximation of the convective term, and it allows us to evaluate the integrals,

$$A_\mathrm{f}(\omega \times \mathbf{u})_\mathrm{f} \cdot \mathbf{n}_\mathrm{f} = -\sum_{\substack{\text{face}\\ \text{nodes}}} \hat{\omega}_\mathrm{n}\mathbf{u}_\mathrm{n} \cdot \{\mathbf{x}_\mathrm{n} - \mathbf{x}_0\} = -\sum_{\substack{\text{face}\\ \text{nodes}}} \hat{\omega}_\mathrm{n}\mathbf{u}_\mathrm{n} \cdot \{\mathbf{x}_\mathrm{n} - \tilde{\mathbf{x}}_\mathrm{f}\}, \tag{74}$$

where $\hat{\omega}_\mathrm{n}$ is the vorticity at the node which is oriented counterclockwise with respect to the face normal. Note that the choice of the position origin, $\tilde{\mathbf{x}}_\mathrm{f}$, is arbitrary. However, it must be the same for both of the nodes touching a particular face.

If the origin (or face position) $\tilde{\mathbf{x}}_\mathrm{f}$ is chosen to be the midpoint between the two cell circumcenters, then Eq. (74) is the expression used in the modified rotational discretization of the convective term (Section 2.2.3). On the other hand, if the face position $\tilde{\mathbf{x}}_\mathrm{f}$ is chosen to be the face midpoint then $\mathbf{x}_\mathrm{n} - \tilde{\mathbf{x}}_\mathrm{f} = \frac{1}{2}A_\mathrm{f}\hat{\mathbf{t}}_\mathrm{f}$ where $\tilde{\mathbf{t}}_\mathrm{f}$ is the tangential vector which points toward the node in question, then

$$A_\mathrm{f}(\omega \times \mathbf{u})_\mathrm{f} \cdot \mathbf{n}_\mathrm{f} = -\frac{1}{2}A_\mathrm{f} \sum_{\substack{\text{face}\\ \text{nodes}}} \omega_\mathrm{n}(\mathbf{v}_\mathrm{n} \cdot \mathbf{t}_\mathrm{f}), \tag{75}$$

which is the expression used in the standard rotational discretization of the convective term (Section 2.2.2).

The two approximations are identical when the mesh is uniform, and both expressions are legitimate first-order accurate approximations for the rotational form of the convective term.

5.2. *Kinetic Energy*

This section analyzes the approximation for the kinetic energy.

We begin with Gauss' Divergence Theorem for an arbitrary bounded volume and vector quantity **f**,

$$\int_{\Omega} \nabla \cdot \mathbf{f}\, dV = \int_{\partial\Omega} \mathbf{f} \cdot \hat{\mathbf{n}}\, dA, \tag{76}$$

where Ω is the volume and $\partial\Omega$ is the boundary of the volume with unit normal vector $\hat{\mathbf{n}}$ oriented outward from the volume. We are actually interested in convex polygonal volumes where Gauss' Theorem simplifies to

$$\int_{\Omega} \nabla \cdot \mathbf{f}\, dV = \sum_{\substack{\text{cell}\\ \text{faces}}} \hat{\mathbf{n}}_{\mathrm{f}} \cdot \int_{\partial\Omega_{\mathrm{f}}} \mathbf{f}\, dA, \tag{77}$$

where $\hat{\mathbf{n}}_{\mathrm{f}}$ is the face normal vector pointing out of the cell in question.

To analyze the accuracy of the kinetic energy approximation set $\mathbf{f} = (\mathbf{u} \cdot \mathbf{r})\mathbf{u}$, where $\mathbf{r} = \mathbf{x} - \mathbf{x}_0$ is the position vector with an arbitrary origin. Then Gauss' Theorem gives

$$\int_{\Omega} \nabla \cdot [(\mathbf{u} \cdot \mathbf{r})\mathbf{u}]\, dV = \sum_{\substack{\text{cell}\\ \text{faces}}} \hat{\mathbf{n}}_{\mathrm{f}} \cdot \int_{\partial\Omega_{\mathrm{f}}} (\mathbf{u} \cdot \mathbf{r})\mathbf{u}\, dA. \tag{78}$$

In Cartesian tensor notation the left-hand side of this equation is written as

$$\int_{\Omega} (u_s r_s u_j)_{,j}\, dV = \int_{\Omega} u_s r_{s,j} u_j\, dV + \int_{\Omega} r_s (u_s u_j)_{,j}\, dV. \tag{79}$$

The gradient of the position vector is the identity matrix ($r_{s,j} = \delta_{sj}$). The equation now becomes

$$\int_{\Omega} \mathbf{u} \cdot \mathbf{u}\, dV + \int_{\Omega} \mathbf{r} \cdot \nabla(\mathbf{uu})\, dV = \sum_{\substack{\text{cell}\\ \text{faces}}} \int_{\partial\Omega_{\mathrm{f}}} (\mathbf{u} \cdot \mathbf{r})\hat{u}\, dA, \tag{80}$$

where $\hat{u}$ is the outward normal component of the velocity at the cell faces. This is an exact equation for polygonal volumes.

Assume that the velocity field **u** is a constant function within the volume. This is a first-order approximation. Then the second term is zero because the velocity is constant and the

integrals can be evaluated:

$$\frac{1}{2}\mathbf{u}\cdot\mathbf{u}V_c = \sum_{\text{faces}}^{\text{cell}} \frac{1}{2}\hat{u}\left(\mathbf{u}\cdot\mathbf{r}_f^{CG}\right)A_f. \tag{81}$$

This is a first-order accurate approximation for the kinetic energy in a cell for arbitrary three-dimensional meshes.

If the mesh is two-dimensional, the face center of gravity is equal to face midpoint. If we choose the origin of the position vector to be the cell circumcenter then $\mathbf{r}_f^{CG} = (\mathbf{x}_f - \mathbf{x}_c^{CG}) = \hat{\mathbf{n}}_f W_f^C$, where W_f^C is the distance between the face and cell circumcenters. Then

$$\frac{1}{2}\mathbf{u}\cdot\mathbf{u}V_c = \sum_{\text{faces}}^{\text{cell}} \frac{1}{2}uuW_f^C A_f, \tag{82}$$

which states that the cell kinetic energy can be approximated by the "kinetic energy" of the normal velocity component summed over the faces. This is the approximation used in the unstructured mesh discretizations schemes when proving conservation of kinetic energy.

5.3. *Interpolation of Velocity to Nodes*

This section looks at the approximation for the velocity vector at the nodes. This velocity is used to calculate the convective term in the rotational discretization. High-order interpolation of velocity to the nodes of distorted quadrilateral meshes was recently discussed by Shashkov *et al.* [24].

We begin with Stokes Theorem for an arbitrary bounded surface and a vector quantity $\mathbf{f}$,

$$\int_S (\nabla\times\mathbf{f})\cdot\mathbf{n}\,dA = \int_{\partial S}\mathbf{f}\cdot\hat{\mathbf{z}}\,dL, \tag{83}$$

where S is a surface with normal $\mathbf{n}$, and ∂S is the boundary of the surface with unit tangential vector $\hat{\mathbf{z}}$ oriented in a counterclockwise direction around the boundary with respect to the face normal. In two dimensions, $\hat{\mathbf{z}}$ points into or out of the plane of interest. Unlike Section 5.1, the polygonal region of interest is *not* the cell faces, but the polygonal region surrounding each node (the Voronoi dual cells). These polygons are planar and Stokes Theorem then becomes

$$\mathbf{z}\cdot\int_S (\nabla\times\mathbf{f})\,dA = \sum_{\text{faces}}^{\text{node}} \hat{\mathbf{n}}_f\cdot\int_{\partial S_f}\mathbf{f}\,dL, \tag{84}$$

where $\hat{\mathbf{n}}_f$ is the unit normal at the face oriented in the counterclockwise direction with respect to the unit node in question, and $\mathbf{z}$ is the vector pointing out of the two-dimensional plane. Set $\mathbf{f} = (\mathbf{a}\cdot\tilde{\mathbf{r}})\mathbf{u}$, where $\tilde{\mathbf{r}} = \mathbf{z}\times\mathbf{r} = \mathbf{z}\times(\mathbf{x}-\mathbf{x}_0)$ is the curl of the position vector with an arbitrary origin, and $\mathbf{a}$ is an arbitrary nonzero constant vector:

$$\mathbf{z}\cdot\int_S (\nabla\times(\mathbf{a}\cdot\tilde{\mathbf{r}})\mathbf{u})\,dA = \sum_{\text{faces}}^{\text{node}} \hat{\mathbf{n}}_f\cdot\int_{\partial S_e}(\mathbf{a}\cdot\tilde{\mathbf{r}})\mathbf{u}\,dL. \tag{85}$$

In Cartesian tensor notation the left-hand side of this equation is written as

$$z_i \int_S \varepsilon_{ijk}(a_s\varepsilon_{snp}z_n r_p u_k)_{,j}\, dA = \int_S \varepsilon_{ijk}\varepsilon_{snp}a_s z_i z_n [u_k r_{p,j} + r_p u_{k,j}]\, dA$$

$$= \int_S [\varepsilon_{jki}\varepsilon_{jsn}a_s z_i z_n u_k + \varepsilon_{snp}a_s z_i z_n r_p \omega_i]\, dA \tag{86}$$

$$= \int_S [(\delta_{ks}\delta_{in} - \delta_{kn}\delta_{is})a_s z_i z_n u_k + a_s z_i \tilde{r}_s \omega_i]\, dA$$

$$= \int_S a_s[u_s - z_s z_n u_n + z_i \tilde{r}_s \omega_i]\, dA. \tag{87}$$

Using the fact that **a** is an arbitrary vector and two dimensionality we can now write that

$$\int_S [\mathbf{u} - \mathbf{z}(\mathbf{z}\cdot\mathbf{u}) + \tilde{\mathbf{r}}(\mathbf{z}\cdot\omega)]\, dA = \int_S \mathbf{u} + \tilde{\mathbf{r}}\omega_n]\, dA = \sum_{\substack{\text{node}\\ \text{faces}}}^{} \mathbf{z} \times \int_{\partial S_e} \mathbf{r}\hat{u}\, dL, \tag{88}$$

where $\hat{u}$ is the component of velocity normal to the face and oriented counterclockwise with respect to the edge tangential vector. This is an exact equation for planar polygons.

Assume that the velocity field **u** is a constant vector on the polygon of interest. This is a first-order approximation. Then the integrals can be evaluated exactly and

$$\mathbf{v}_n A_n = \mathbf{z} \times \sum_{\substack{\text{node}\\ \text{faces}}}^{} \{\mathbf{x}_f^* - \mathbf{x}_n\}\hat{u} W_f, \tag{89}$$

where $\mathbf{x}_f^*$ is the midpoint between the two cell circumcenters. This is the edge velocity reconstruction used in the modified rotational discretization.

On a uniform mesh the face midpoint is the same as the face circumcenter and $\{\mathbf{x}_f^* - \mathbf{x}_n\} = D_{nf}\hat{\mathbf{n}}_f \times \mathbf{z}$ where D_{nf} is the distance between the node and face center. Then

$$\mathbf{v}_n A_n = -\mathbf{z} \times \left[\mathbf{z} \times \sum_{\substack{\text{node}\\ \text{faces}}}^{} D_{nf}\mathbf{n}_f u W_f\right] = \sum_{\substack{\text{node}\\ \text{faces}}}^{} W_f D_{nf}\mathbf{n}_f u, \tag{90}$$

which is the interpolation used in the standard rotational discretization. Note that the orientation of the face normal and normal velocity component are now arbitrary as long as they are consistent with each other.

5.4. *Interpolation of Velocity to Cells*

This section looks at the approximation for the cell velocity vector.

We begin with Gauss' Divergence Theorem for an arbitrary bounded polyhedral volume and a vector quantity **f**,

$$\int_\Omega \nabla\cdot\mathbf{f}\, dV = \sum_{\substack{\text{cell}\\ \text{faces}}}^{} \hat{\mathbf{n}}_f \cdot \int_{\partial\Omega_f} \mathbf{f}\, dA, \tag{91}$$

where Ω is the volume and $\partial\Omega$ is the boundary of the volume with unit normal vector $\hat{\mathbf{n}}$

oriented outward from the volume. Now set $\mathbf{f} = (\mathbf{a} \cdot \mathbf{r})\mathbf{u}$, where $\mathbf{r} = \mathbf{x} - \mathbf{x}_0$ is the position vector with an arbitrary and $\mathbf{a}$ is an arbitrary nonzero constant vector. Then Gauss' Theorem gives

$$\int_S \nabla \cdot [(\mathbf{a} \cdot \mathbf{r})\mathbf{u}]\, dV = \sum^{\substack{\text{cell}\\ \text{faces}}} \hat{\mathbf{n}}_f \cdot \int_{\partial\Omega_f} (\mathbf{a} \cdot \mathbf{r})\mathbf{u}\, dA. \tag{92}$$

In Cartesian tensor notation the left-hand side of this equation is written as

$$\int_\Omega (a_s r_s u_j)_{,j}\, dV = a_s \int_\Omega r_{s,j} u_j\, dV + a_s \int_\Omega r_s u_{j,j}\, dV. \tag{93}$$

The gradient of the position vector is the identity matrix ($r_{sj} = \delta_{sj}$), and since $\mathbf{a}$ is an arbitrary vector,

$$\int_\Omega \mathbf{u}\, dV + \int_\Omega \mathbf{r}(\nabla \cdot \mathbf{u})\, dV = \sum^{\substack{\text{cell}\\ \text{faces}}} \int_{\partial\Omega_f} \hat{u}\mathbf{r}\, dA, \tag{94}$$

where $\hat{u}$ is the outward normal component of the velocity at the cell faces. This is an exact equation for polygonal volumes.

Assume that the velocity field $\mathbf{u}$ is a constant function (a first-order approximation). Then the second term will be zero and the integrals can be evaluated:

$$\mathbf{u}V_c = \sum^{\substack{\text{cell}\\ \text{faces}}} \hat{u}\mathbf{r}_f^{CG} A_f. \tag{95}$$

This is the interpolation expression for the cell velocity vector used in the modified discretization schemes.

If the mesh is two-dimensional then the face center of gravity is equal to face circumcenter. Allow the origin of the position vector to be the cell circumcenter then $\mathbf{r}_f^{CG} = (\mathbf{x}_f^{CC} - \mathbf{x}_c^{CC}) = \hat{\mathbf{n}}_f D_{ef}$ where D_{ef} is the distance between the face and cell circumcenters. This results in the expression

$$\mathbf{u}V_c = \sum^{\substack{\text{cell}\\ \text{faces}}} u\mathbf{n}_f D_{ef} A_f, \tag{96}$$

which is a first-order approximation relating the cell velocity vector to the normal velocity components at the faces. The orientation of the normal vector and normal velocity are now arbitrary as long as they are mutually consistent.

5.5. *Numerical Tests of Accuracy*

This section confirms the accuracy assessments of the preceding sections using a series of numerical tests. In each case, an exact sinusoidal function is assigned to the input variables. The exact solution is computed analytically and the approximate solution is computed numerically. Rather than changing the mesh size, which is 6200 triangles, mesh refinement has been performed by changing the wavelength of the input variables. Small wavelengths are equivalent to a coarse mesh solution.

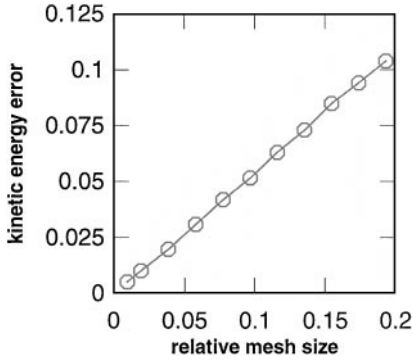

FIG. 6. Error in the discrete kinetic energy approximation (Eq. (82)) as a function of mesh size. First-order accuracy is obtained.

The exact streamfunction was set to be $\frac{100}{2\pi N}\sin(2\pi N x/100)\cos(2\pi N y/100)$ on a domain which was a 100×100 square. Exact velocities and vorticity were then derived from this streamfunction. The maximum velocity magnitude is unity. The average mesh spacing was calculated assuming equilateral triangles cover the domain and was found to be 1.93. The effective length of the domain is $100/N$, where N is a variable integer value. Larger values of N correspond to a coarser effective mesh. The relative mesh size is defined to be $\Delta x_{\text{average}}/L_{\text{effective}} = 0.193N$. So a relative mesh size of 0.2 corresponds to roughly five cells per wavelength.

Figure 6 shows a plot of the rms error of the kinetic energy as a function of relative mesh size when the kinetic energy is calculated using Eq. (82). The exact kinetic energy was calculated at cell circumcenters, but evaluating the exact kinetic energy at the cell center of gravity makes only about 1% difference in the results. The average kinetic energy for this flow field is 0.25. The approximation given by Eq. (82) is clearly first-order accurate.

The approximation for the convective term is was tested by assuming exact vorticity and velocity at the mesh nodes, and using Eq. (74) to calculate the normal component of $\omega \times \mathbf{u}$ at the faces. The standard rotational discretization (Eq. (75)) is shown in Fig. 7 by triangles. It is second-order accurate which is not surprising since this equation is essentially a midpoint average when applied in two-dimensions. However, it was found that this form of the interpolation requires a velocity interpolation which is zeroth-order accurate (see Fig. 8)

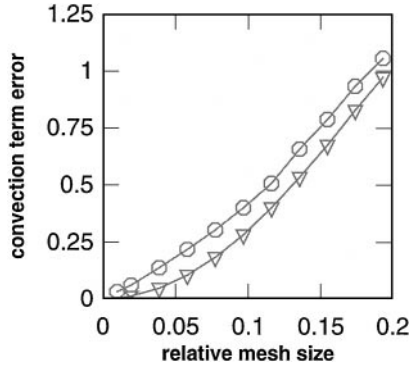

FIG. 7. Error in the rotational convection term (Eq. (74)) as a function of mesh size. Triangles are the standard discretization, and circles are the modified discretization.

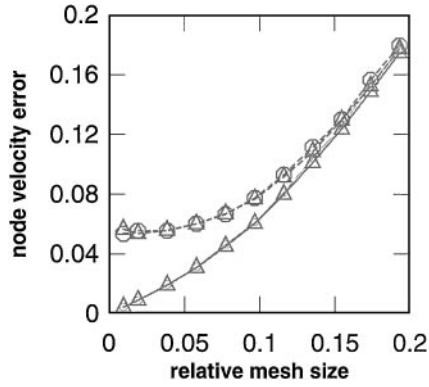

FIG. 8. Error in the node velocity (Eq. (89)) as a function of mesh size. Circles are error in u, and triangles are the error in v. The dashed lines are the standard interpolation scheme and the solid lines are the first-order modified interpolation scheme.

if kinetic energy is to be conserved. The modified convective term, shown with circles and described in Section 2.2.3, is first-order accurate and results in a velocity interpolation which is also first-order accurate.

Figure 8 shows the accuracy of the velocity interpolation (Eq. (89)) to the nodes. Circles are the error in the x component of velocity and triangles are the error in the y component. The dashed lines represent the error in the velocity interpolation required by the standard rotational form (Eq. (90)). For coarse meshes it is roughly the same as the modified interpolation scheme, but as the mesh is refined it does not converge to zero error. The solid lines are the modified interpolation scheme which is shown to be first-order accurate.

The error in the approximation for the cell velocity (Eq. (96)) is evaluated in Fig. 9. Again, the circles are the error in the x component of velocity and the triangles are the error in the y component. The approximation is shown to be first-order accurate.

It was also confirmed that the modified velocity approximation at the nodes and the velocity approximation at the cells are exact for constant velocity fields.

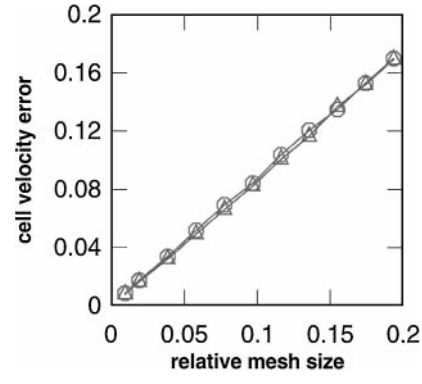

FIG. 9. Error in the cell velocity (Eq. (96)) as a function of mesh size. Circles are error in u, and triangles are the error in v.

6. DISCUSSION

It has been shown both theoretically and numerically that unstructured staggered mesh schemes can be constructed in two dimensions which conserve kinetic energy, vorticity, and momentum. Mass conservation is a trivial consequence of the mesh staggering, but these other conservation properties are not as immediately obvious.

The primary unknowns of the staggered mesh scheme are the velocity components normal to cell faces, and the precise approximations that are used to approximate secondary unknowns, such as velocity vectors or kinetic energy, are critical to achieving the conservation properties of the scheme. This paper has demonstrated both how the appropriate approximations can be derived during the course of the conservation proof and also how the accuracy of the resulting approximations can be rigorously evaluated (Section 5).

In particular, it has been shown that discretizations of the rotational form of the Navier–Stokes equations can conserve kinetic energy and vorticity to machine precision. Discretizations of the divergence form of the equations can conserve kinetic energy and momentum. It was also shown that certain discretizations require nonconvergent interpolations in order to be conservative, but that these discretizations can be modified to maintain conservation properties without jeopardizing the convergence.

There are many other possible staggered mesh discretizations. A number have already been presented in the literature. The proofs presented herein do not preclude the possibility that other staggered mesh schemes are also conserving. It is anticipated that the examples provided in Sections 2 and 3 and the tools developed in Section 5 will allow the reader to analyze the conservation properties of other staggered mesh schemes which might be of particular interest.

ACKNOWLEDGMENTS

This work was supported, in part, by the Center for Integrated Turbulence Simulation at Stanford University which is supported by a Department of Energy ASCI grant. Most of the proofs were formulated while the author was employed at Aquasions Inc. Their support is gratefully acknowledged. I would also like to thank Charles Pierce for his many helpful conversations on this subject.

REFERENCES

1. F. H. Harlow and J. E. Welch, Numerical calculations of time dependent viscous incompressible flow of fluid with a free surface, *Phys. Fluids* **8**, 2182 (1965).
2. D. K. Lilly, On the computational stability of numerical solutions of time-dependent non-linear geophysical fluid dynamics problems, *Mon. Weather Rev.* **93**(1), 11 (1965).
3. J. B. Perot, Direct numerical simulation of turbulence on the Connection Machine, *Parallel Computational Fluid Dynamics '92*, edited by R. B. Pelz, A. Ecer, and J. Hauser (North-Holland, Amsterdam, 1993).
4. Y. Na and P. Moin, Direct numerical simulation of turbulent boundary layers with adverse pressure gradient and separation, *Report TF-28* (Thermosciences Division, Dept. of Mech. Eng., Stanford University, Stanford, CA, 1996).
5. H. Le, P. Moin, and J. Kim, Direct numerical simulation of turbulent flow over a backward facing step, *J. Fluid Mech.* **330**, 349 (1997).
6. K. Akselvoll and P. Moin, Large eddy simulation of turbulent confined coannular jets, *J. Fluid Mech.* **315**, 387 (1996).
7. R. Mittal and P. Moin, Suitability of upwind-biased finite difference schemes for large-eddy simulation of turbulent flows, *AIAA J.* **35**(8), 1415 (1998).

8. Y. V. Apanovich and E. D. Lyumkis, Difference schemes for the Navier–Stokes equations on a net consisting of Dirichlet cells, U.S.S.R. *Comput. Maths. Math. Phys.* **28**(2), 57 (1988).
9. K. Jansen, Large-eddy simulation of flow around a NACA 4412 airfoil using unstructured grids, in *Center for Turbulence Research Annual Research Briefs* (1996), Stanford/NASA-Ames, p. 225.
10. C. A. Hall, J. S. Peterson, T. A. Porsching, and F. R. Sledge, The dual variable method for finite element discretizations of Navier/Stokes equations, *Int. J. Numer. Methods Eng.* **21**, 883 (1985).
11. R. A. Nicolaides, Direct discretization of planar div-curl problems. ICASE Report 89-76 (1989).
12. R. A. Nicolaides, The covolume approach to computing incompressible flow, *Incompressible Computational Fluid Dynamics*, edited by M. D. Gunzburger and R. A. Nicolaides (Cambridge Univ. Press, Cambridge, UK, 1993), p. 295.
13. R. A. Nicolaides and X. Wu, *Covolume Solutions of Three-Dimensional Div-Curl Equations* (1995), ICASE Report. 95-4.
14. F. Bertagnolio and O. Daube, Solution of the div-curl problem in generalized curvilinear coordinates, *J. Comput. Phys.* **138**, 121 (1997).
15. J. M. Hyman and M. Shashkov, The orthogonal decomposition theorems for mimetic finite difference methods, *SIAM J. Numer. Anal.* **36**(3), 788 (1999).
16. J. M. Hyman and M. Shashkov, Mimetic discretizations of Maxwells equations, *J. Comput. Phys.* **151**, 881 (1999).
17. Y. Morinishi, T. S. Lund, O. V. Vasilyev, and P. Moin, Fully conservative higher order finite difference schemes for incompressible flow, *J. Comput. Phys.* **143**, 90 (1998).
18. J. M. Hyman, R. J. Knapp, and J. C. Scovel, High order finite volume approximations of differential operators on nonuniform grids, *Physica D* **60**, 112 (1992).
19. C. A. Hall, J. C. Cavendish, and W. H. Frey, The dual variable method for solving fluid flow difference equations on Delaunay triangulations, *Comput. Fluids* **20**(2), 145 (1991).
20. A. Lippolis, G. Vacca, and B. Grossman, Incompressible Navier–Stokes solutions on unstructured grids using a co-volume technique, in *13th International Conference on Numerical Methods in Fluid Dynamics*, edited by M. Napolitano and F. Sabetta (Springer-Verlag, Amsterdam, 1992), p. 270.
21. J. C. Cavendish, C. A. Hall, and T. A. Porsching, A complementary volume approach for modelling three-dimensional Navier–Stokes equations using dual Delaunay/Voronoi tessellations, *Int. J. Numer. Methods Heat Fluid Flow* **4**, 329 (1994).
22. R. A. Nicolaides, The covolume approach to computing incompressible flows, in *Algorithmic Trends in Computational Fluid Dynamics*, edited by M. Y. Hussaini, A. Kumar, and M. D. Salas (Springer-Verlag, Amsterdam, 1993).
23. S. H. Chou, Analysis and convergence of a covolume method for the generalized Stokes problem, *Math. Comput.* **66**(217), 85 (1997).
24. M. Shashkov, B. Swartz, and B. Wendroff, Local reconstructuin of a vector field from its normal components on the faces of grid cells, *J. Comput. Phys.* **139**, 406 (1998).